

Hamiltonian Hopf bifurcations and dynamics of NLS/GP standing-wave modes

Roy Goodman

Department of Mathematical Sciences, New Jersey Institute of Technology, Newark, NJ 07102, USA

E-mail: goodman@njit.edu

Received 31 January 2011, in final form 25 August 2011


Published 30 September 2011

Online at stacks.iop.org/JPhysA/44/425101

Abstract

We examine the dynamics of solutions to nonlinear Schrödinger/Gross–Pitaevskii equations that arise due to semisimple indefinite Hamiltonian Hopf bifurcations—the collision of pairs of eigenvalues on the imaginary axis. We construct localized potentials for this model which lead to such bifurcations in a predictable manner. We perform a formal reduction from the partial differential equations to a small system of ordinary differential equations. We analyze the equations to derive conditions for this bifurcation and use averaging to explain certain features of the dynamics that we observe numerically. A series of careful numerical experiments are used to demonstrate the phenomenon and the relations between the full system and the derived approximations.

PACS numbers: 05.45.Ac, 02.30.Oz, 42.65.Sf, 42.65.Wi, 67.85.Hj

 Online supplementary data available from stacks.iop.org/JPhysA/44/425101/mmedia

(Some figures may appear in colour only in the online journal)

1. Introduction

This paper brings together several threads in the study of nonlinear waves in media with a localized defect. It focuses on one specific example: the dynamics of low-amplitude solutions to the nonlinear Schrödinger/Gross–Pitaevskii (NLS/GP) equation

$$i\partial_t u = Hu - |u|^2 u; \quad H = -\partial_x^2 + V(x), \quad (1.1)$$

in the presence of an oscillatory instability, arising from a particular type of Hamiltonian Hopf (HH) bifurcation. Our interest in this problem has four primary motivations. In the remainder of this section, we discuss these motivations, while simultaneously defining the mathematical problem to be studied.

1.1. *Physical motivation*

In nonlinear optics, equation (1.1) describes the evolution of the envelope $u(x, t)$ of an electromagnetic field E inside a nonlinear waveguide [1, 2]. The equation is derived using the paraxial approximation, so that t measures the propagation distance along the waveguide axis, and x the transverse profile. The waveguide is assumed to be thin in the third (y) direction, so that variation in this direction can be safely ignored. The potential $V(x)$ represents the waveguide structure. The material is assumed to be Kerr nonlinear, i.e. a nonzero electric field E locally and quadratically modifies the refractive index, $n = n_0 + n_2(|E|^2)$.

When the sign on the nonlinear term of (1.1) is reversed, it describes the evolution of a Bose–Einstein condensate (BEC), a state of matter achievable at extreme low temperatures in which atoms lose their individual identities and are described by a common wavefunction [3]. For equation (1.1) to hold, the three-dimensional condensate must be strongly confined by a steep potential in the two transverse directions y and z so that it assumes a ‘cigar’ shape. The term $V(x)$ then describes a less steeply confining potential in the third spatial dimension.

1.2. *Mathematical motivation—moving from stability to dynamics*

A fundamental object of study for systems like (1.1) is a nonlinear standing wave or bound state, i.e. a localized solution to (1.1) of the form

$$u(x, t) = e^{-i\Omega t} U(x).$$

A solution consists of a function $U(x) \in H^2$, and real numbers Ω and \mathcal{N} satisfying

$$\begin{aligned} \Omega U &= HU - U^3; \\ \int_{-\infty}^{\infty} U^2(x) dx &= \|U\|_2^2 = \mathcal{N}. \end{aligned} \tag{1.2}$$

The parameter $\mathcal{N} > 0$ represents the number of particles of a BEC or the total intensity of the light in optics. This solution is a nonlinear generalization of an eigenfunction of a linear Schrödinger equation, although the principle of superposition does not apply. There exist continuous families of solutions to (1.2) that are indexed by the intensity \mathcal{N} . Some of these families persist in the limit $\mathcal{N} \rightarrow 0$, and approach the eigenpairs of the linear system. We denote the nonlinear continuation of the linear eigenfunction $U_j(x)$ as $U_j^{\mathcal{N}}(x)$.

Nonlinear bound states, or standing waves, represent coherent and simple states that should be observable in a laboratory experiment. Such bound states may be found numerically, or, for certain potentials $V(x)$, computed exactly in the linear limit and perturbatively for $\mathcal{N} \ll 1$. For such states to be observable in experiments, they must be stable, i.e. if a solution to equation (1.1) is initialized at $t = 0$ with value close to, but not equal to, a solution to system (1.2), then it must stay in a neighborhood of that solution for all $t > 0$.

The stability of such solutions has been widely studied, especially their spectral stability. Eigenvalues or continuous spectrum with positive real part in the linearization of (1.1) about a given solution is a sufficient condition for instability. The intensity \mathcal{N} becomes a bifurcation parameter: as \mathcal{N} changes a particular solution may become unstable, and in addition the number of solutions and the dynamics may change. The systems can change in a small number of ways—bifurcation types—dependent on the leading order linear and nonlinear terms of the system in a neighborhood of the bifurcation, their normal forms.

Recent studies have examined possible bifurcations in system (1.1) and related systems. Several groups have demonstrated, for example, that solutions to (1.2) with a double-well potential,

$$V_L^{(2)}(x) = \tilde{V}(x - L) + \tilde{V}(x + L) \quad \text{with} \quad \tilde{V}(-x) = \tilde{V}(x), \tag{1.3}$$

undergo a symmetry-breaking (SB) bifurcation as the parameter \mathcal{N} is raised from zero [4, 5]. At a critical value \mathcal{N}_{SB} , a symmetric solution to equation (1.2) loses stability and two stable, asymmetric standing wave modes are created. This has been subsequently understood in work focusing on the time-dependent dynamics that arise near the bifurcation [6, 7], where the dynamics of the Duffing equation are seen. The main tool for studying the dynamics in all the above references, and here too, is to derive a system of Hamiltonian ordinary differential equations (ODEs) whose dynamics approximate those of system (1.1).

Kapitula, Kevrekidis and Chen [8] have shown that for a triple-well potential

$$V_L^{(3)}(x) = \tilde{V}(x-L) + \tilde{V}(x) + \tilde{V}(x+L) \quad \text{with} \quad \tilde{V}(-x) = \tilde{V}(x), \quad (1.4)$$

that this symmetry-breaking bifurcation is replaced by three separate saddle-node bifurcations, which give rise to six additional families of standing waves. They numerically investigated the stability of all these solutions but did not address the nonlinear dynamics, which is the subject of this paper.

1.3. Mathematical motivation—from simple to complex dynamics

The SB bifurcation studied by Kirr *et al* was shown by Marzuola and Weinstein to display the dynamics typical of such systems. Below the bifurcation, the ODE system has a single-well potential energy, and thus a one-parameter family of periodic orbits. Above the bifurcation, the potential energy has a dual-well shape and three topologically distinct families of periodic orbits. This manifests itself in a wobbling of the shape of the asymmetric solutions or a periodic exchange of energy between the two wells [6]; see also [7, 9].

The SB bifurcation studied above is the simplest that can be found in Hamiltonian partial differential equations (PDEs) with symmetries. The equations derived are integrable, and the phase plane in the reduced ODE can take one of four simple arrangements, corresponding to subcritical and supercritical bifurcations. Here, we focus on the next simplest bifurcation, a relative of the HH bifurcation, which requires one more degree-of-freedom and gives rise to dynamics that appear to be non-integrable and chaotic. This requires a potential more similar to (1.4) than to (1.3). The dynamics require certain resonance assumptions on the spectrum of $V(x)$, which we outline below.

1.4. Mathematical motivation—analyzing previous simulations

There are several types of HH bifurcation, which have been seen in numerical simulations of a variety of physical systems that support nonlinear waves. These bifurcations arise due to ‘Krein collisions’ between frequencies, defined in section 4.4 below. Such a bifurcation is observed numerically in the spectrum of the linearization of (1.1) about a certain standing wave, when the potential (1.4) is used [8, figure 6(d)]; see also [10]. Although such a bifurcation is commonly referred to as an HH bifurcation in the nonlinear wave literature, the analysis below shows it to be, more precisely, a semisimple Hopf bifurcation, corresponding a semisimple 1:−1 resonance defined below in equation (2.8).

Several studies have demonstrated numerically the existence of Krein collisions in other NLS-related settings: in discrete wave equations [11–14] and in BECs [15–18]. In these, the bifurcation is discussed only in the context of detecting the instability transition in the linear spectrum, or by performing a small number of numerical solutions to the initial value problem. Theocharis *et al* [19] present one such simulation of multiple dark solitons in a BEC system. They describe the Krein collision as ‘the collision of the second anomalous mode with the quadrupole mode’ and display dynamics in their figure 5(c) very much like our

figure 6(b), column 3. A goal of this paper is to shed light on the origin of such patterns in this and similar numerical simulations.

Many of these references cite in passing the monograph of van der Meer [20], but this analysis only applies to the generic HH bifurcation, and not the semisimple cases. In both bifurcations, the linearization matrix possesses a complex-conjugate pair of multiplicity-two imaginary eigenvalues. In the semisimple case, the corresponding block of the linearization can be diagonalized over \mathbb{C} . In the generic case, this block has a non-trivial Jordan form. The bifurcation in the generic HH case is codimension-one and very well understood; see, for example, [20–23]. By contrast, the bifurcation discussed in this paper has codimension three.

Kapitula *et al* have developed rigorous analytical methods for detecting Krein collisions in Hamiltonian nonlinear wave equations [24, 25], and apply these methods to study the stability of many different solutions. In [26], they use this machinery to study the stability of rotating matter waves in Bose–Einstein condensates, and demonstrate the presence of Krein collisions. They supplement this with well-chosen numerical simulations showing the dynamics that arise when the solution is destabilized.

Overview and organization of the paper

In this paper, we focus the dynamics in the vicinity of an HH bifurcation. The main tool of the paper is to derive a finite-dimensional model of the dynamics, via a Galerkin truncation. This Hamiltonian system of ODEs is then further reduced via symmetries to a two degree-of-freedom system, the smallest that can possess a $1 : -1$ resonance. Using Hamiltonian averaging methods, we are able to separate further the slow and fast timescales of this reduced system. Using these tools, we focus on the instability of one particular solution to (1.1) and the dynamics nearby. We use numerical simulations to show the agreement between the different models, and to demonstrate the appearance of chaotic dynamics.

Section 2 contains preliminaries. After a brief list of notation used, we discuss in section 2.2 technical assumptions on the potential $V(x)$. After a slight reformulation of the problem in section 2.3, we review some basic concepts from dynamical systems and Hamiltonian mechanics in section 2.4. Section 3 discusses the elementary properties of the finite-dimensional model. In section 3.1, we briefly describe its derivation from (1.1) and in section 3.2 we use symmetry to reduce the dimension from three to two. We compute a further reduction of the dimension to (3.10), using Hamiltonian averaging to put the system in Gustavson normal form. In sections 4 and 5, we discuss the stability of certain solutions, and the dynamics in a neighborhood of those solutions. Section 4 contains analysis and section 5 a numerical study. Section 4.1 reviews the known stationary solutions of system (3.4). In section 4.2 and in section 4.3, we compute the linearizations of the PDE and the ODE about the relevant solutions, and in section 4.4, we derive an analytical approximation to the amplitude at which the antisymmetric mode becomes unstable. In section 4.5, we describe the phase space of the one degree-of-freedom averaged equations. Section 5 contains numerical experiments that further explore the phase space, and compare the results of simulations of the different approximations. Section 5.1 compares the stability result of section 4.4 with direct simulations of the linearized problem defined in section 4.2. Section 5.2 compares the numerically computed dynamics of NLS/GP and the finite-dimensional model. Section 6 contains a concluding discussion and presents several directions for planned future research. In the appendix, we sketch the construction the potential, thus proving the existence of a potential satisfying the assumptions of section 2.2, while leaving further details to the supplementary materials (available at stacks.iop.org/JPA/44/425101/mmedia).

2. Preliminaries

2.1. Notation

- An overbar, \bar{z} represents the complex conjugate of z .
- $\Re z = \text{Real}(z)$ and $\Im z = \text{Imag}(z)$.
- $\langle f, g \rangle = \int_{\mathbb{R}} f(x)\bar{g}(x) dx$ is the L^2 inner product over complex-valued L^2 functions of a real argument.
- The inner product of $u, v \in \mathbb{R}^n$ is $\langle u, v \rangle = \sum_{k=1}^n u_k v_k$ and in \mathbb{C}^n is $\langle u, v \rangle = \sum_{k=1}^n u_k \bar{v}_k$.

2.2. Assumptions on the potential $V(x)$ and the spectrum of H

We make the following assumptions about $V(x)$ and about the frequencies Ω_j that solve the linear eigenvalue problem

$$HU_j(x) = \Omega_j U_j(x). \quad (2.1)$$

Assumptions on spectrum

- (S1) $\Omega_1 < \Omega_2 < \Omega_3 < 0$;
 (S2) $\Omega_2 - \Omega_1 = O(1)$;
 (S3) $\Omega_3 - \Omega_2 = O(1)$;
 (S4) $(\Omega_3 - \Omega_2) - (\Omega_2 - \Omega_1) \ll 1$;
 (S5) $2\Omega_2 - \Omega_1 < 0$;

Assumptions on potential

- (V1) $V(x) < 0$;
 (V2) $\lim_{|x| \rightarrow \infty} V(x) = 0$;
 (V3) $V(x) = V(-x)$.

To satisfy assumption (S4) in particular, we let

$$\Omega_2 - \Omega_1 = W - \epsilon \quad \text{and} \quad \Omega_3 - \Omega_2 = W + \epsilon, \quad (2.2)$$

where $\epsilon \ll W$ and $W = O(1)$. The sign of ϵ is left unspecified while $W > 0$. Assumption (S5) ensures that the linearization about mode u_2 possesses no leading-order resonances between the discrete and continuous spectrum. The evenness assumption assures that the eigenfunctions u_j are, alternately, even and odd functions, and we further assume they satisfy $\|U_j\| = 1$. Note further that, by [27, theorem 13.9], the essential spectrum consists entirely of continuous spectrum; specifically

$$\sigma_{\text{ess}} = [0, \infty).$$

Remark 1. As in [4], these assumptions ensure that equation (1.1) has $O(2) \times \mathbb{Z}_2$ symmetry, as does the finite-dimensional system that we derive.

Kirr *et al* show that for a similar system with a symmetric potential with only two closely spaced eigenvalues and $\Omega_2 - \Omega_1 \ll 1$, that the SB bifurcation of the nonlinear continuation of $U_1^{\mathcal{N}}$ occurs at a small intensity

$$\mathcal{N} \propto \Omega_2 - \Omega_1.$$

Analogously, we show in this paper that under the above assumptions, the Krein collision, in the linearization about $U_2^{\mathcal{N}}$ occurs for

$$\mathcal{N} \propto \Omega_3 - 2\Omega_2 + \Omega_1 \propto |\epsilon|.$$

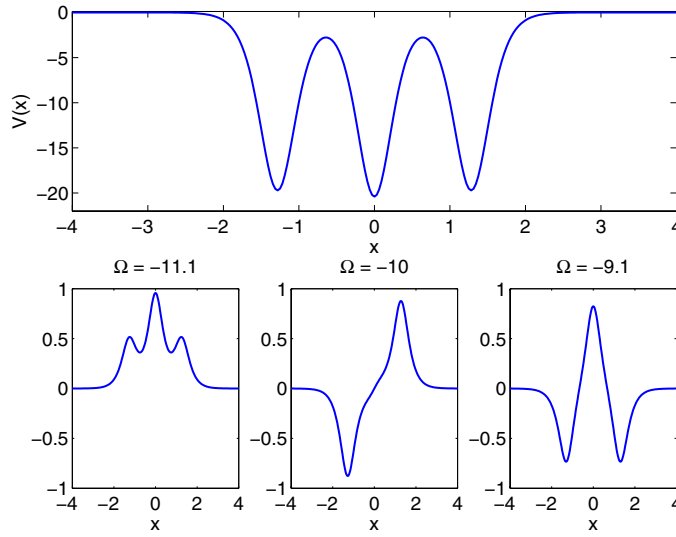


Figure 1. Top: the potential with $\Omega_2 = -10$, $W = 1$ and $\epsilon = -0.1$ in assumption 2.2. Bottom: its corresponding eigenfunctions.

In the appendix, we demonstrate a potential $V(x)$ with two prescribed negative eigenvalues and which also satisfies conditions (V1)–(V3). A similar potential with three frequencies is derived in the supplementary materials (available at stacks.iop.org/JPA/44/425101/mmedia). An example constructed in this manner and satisfying the above assumptions is shown in figure 1. The potential is chosen such that $\Omega = (-11.1, -10, -9.1)$. The numerical computations in the paper use this potential, except where noted. It is the odd mode U_2^N , the nonlinear continuation of eigenfunction U_2 , that undergoes the HH bifurcation.

Remark 2. In the two-mode case, breaking assumption (V3) causes the bifurcation to degenerate from a pitchfork bifurcation to a saddle node. In the three-mode case, the Krein collision is generic and occurs regardless of this assumption, although the type of HH bifurcation may change. Still, assumption (V3) greatly reduces the number and complexity of the nonlinear terms in the reduced system.

2.3. An alternate formulation

The change of variables $u = \sqrt{\mathcal{N}}\tilde{u}$ in equation (1.1) and $U = \sqrt{\mathcal{N}}\tilde{U}$ in (1.2) produces the modified evolution equation

$$i\partial_t \tilde{u} = H\tilde{u} - \mathcal{N}|\tilde{u}|^2 \tilde{u}, \tag{2.3}$$

and stationary equations

$$\begin{aligned} \Omega \tilde{U} &= H\tilde{U} - \mathcal{N}\tilde{U}^3; \\ \int_{-\infty}^{\infty} \tilde{U}^2(x) dx &= \|\tilde{U}\|_2^2 = 1. \end{aligned} \tag{2.4}$$

This formulation presents a natural environment for studying the $\mathcal{N} \rightarrow 0$ limit. Since this system is well-defined regardless of $\text{sign}(\mathcal{N})$, we can study all the bifurcations for $\mathcal{N} \in \mathbb{R}$, which gives a fuller picture of the dynamics, unifying the focusing and defocusing NLS equations. We use this formulation for the remainder of the paper.

Remark 3. This formulation has, in general, no bifurcation at $\mathcal{N} = 0$: for almost all potentials $V(x)$, a smooth family of functions passes through any solution to system (2.4) at $\mathcal{N} = 0$.

2.4. *Hamiltonian systems, resonance and stability*

The principal tool of this paper is to formally reduce system (2.3) to a finite-dimensional system. While the definitions given in this section refer to finite-dimensional systems, equivalent definitions exist for infinite-dimensional systems.

It is convenient to define the Hamiltonian in terms of n complex variables $z = (z_1, z_2, \dots, z_n)$ and their complex conjugates. In this setting, the Hamiltonian H is a real valued function $H(z, \bar{z})$ with canonical position vector given by $q = z$ and momentum vector by $p = i\bar{z}$. The evolution equations are

$$i \frac{d}{dt} z_j = \frac{\partial}{\partial z_j^*} H(z, \bar{z}); \quad j = 1, \dots, n. \tag{2.5}$$

We often make reference to a ‘solution’ to a Hamiltonian $H(z, \bar{z})$, by which we mean a solution to the associated system (2.5).

2.4.1. *Relative equilibria and relative periodic orbits.* A solution to system (2.5) of the form

$$z = e^{-i\Omega t} z_0,$$

i.e. a solution that is time-invariant in an appropriate rotating reference frame, is known as a *relative equilibrium*. Equation (2.4) describes such relative equilibria for NLS/GP (2.3). Similarly, a *relative periodic orbit* is a quasi-periodic orbit which appears periodic when viewed in an appropriate rotating reference frame. A more technical definition of a relative equilibrium (or periodic orbit) is a solution to (2.5) that corresponds to an equilibrium (or periodic orbit) of a symmetry-reduced Hamiltonian derived from (2.5).

2.4.2. *Quadratic Hamiltonian systems and resonances.* A more standard formulation is to make the change of variables $q = (z + \bar{z})/\sqrt{2}$; $p = (z - \bar{z})/(i\sqrt{2})$, which is canonical, i.e. it preserves the Hamiltonian structure $\dot{q}_j = \partial H/\partial p_j$ and $\dot{p}_j = -\partial H/\partial q_j$. Writing $x = \begin{pmatrix} q \\ p \end{pmatrix}$, the equations of motion are $\frac{d}{dt} x = J\nabla H$; $J = \begin{pmatrix} 0 & I \\ -I & 0 \end{pmatrix}$.

Assuming that $x = 0$ is an equilibrium, then $H = H_2(x) + O(|x|^3)$, where $H_2(x) = \langle x, Kx \rangle$ for some symmetric matrix K . The linear stability of the trivial solution is determined by the eigenvalues λ_j of the matrix JK . The real and imaginary parts of the eigenvalues determine, respectively, the growth and decay rates of the solution, and the oscillation frequency of small solutions. The solution is unstable if any eigenvalues λ_j satisfy $\Re \lambda_j > 0$.

If the trivial solution is neutrally linearly stable, then JK has n complex conjugate pairs of eigenvalues $\lambda = \pm i\Omega_j$ on the imaginary axis, the natural frequencies of the system. If these eigenvalues are distinct and nonzero, then the matrix JK is diagonalizable. Any solution to the linear system is of the form

$$x = \sum_{j=1}^n \Re(c_j e^{-i\Omega_j t} V_j), \tag{2.6}$$

where V_j is an eigenvector corresponding to $i\Omega_j$.

Topologically, such a solution lies on an n -dimensional torus \mathbb{T}^n in the $2n$ -dimensional phase space. The analysis in this paper requires some understanding of resonances in Hamiltonian systems, see e.g. Wiggins [28]. A *resonance relation* is a solution to the equation

$$\langle k, \Omega \rangle = 0 \quad \text{with } k \in \mathbb{Z}^n \setminus \{0\}. \tag{2.7}$$

The sum

$$|k| = \sum_{j=1}^n |k_j|$$

defines the order of a given resonance; e.g. a frequency vector Ω satisfying assumption 2.2 with $\epsilon = 0$, together with the vector $k = (1, -2, 1)$, satisfies equation (2.7) and defines a resonance of order 4. The number of linearly independent vectors k that solve equation (2.7) is the *multiplicity* of the resonance. In the absence of such resonances, each solution (2.6) is dense on \mathbb{T}^n . Given a resonance with multiplicity m , the solutions are confined to, and dense on, $(n - m)$ -dimensional subsets of \mathbb{T}^n which are themselves topologically equivalent to \mathbb{T}^{n-m} . To understand this, think of the two-dimensional case. If there are two non-resonant frequencies, any nonzero solution is dense on a two-torus, so its closure is two-dimensional, but if the two frequencies are rationally related, then each one-dimensional orbit is closed. The closed orbits lie on the level sets of an additional conservation law within \mathbb{T}^2 . A system with a near-resonance, $\langle k, \Omega \rangle \ll 1$ but non-zero, and small nonzero nonlinear terms will have a nearly conserved quantity. Averaging methods then allow us to decrease the dimension of the system and obtain simpler equations that accurately approximate solutions for long but finite times.

While our procedure is to first derive a finite-dimensional Hamiltonian approximation to NLS and apply averaging methods to analyze this finite-dimensional system, Bambusi and collaborators have applied such methods directly to a variety of PDE systems [29–31], the most relevant being [32]. We return to this theme in the conclusion, after more of the technical details have been introduced.

2.4.3. Bifurcations. Bifurcation points, locations in parameter space where the stability, type, or number of solutions changes may be classified into different types, or normal forms. A normal form for a system of differential equations is any equivalent system of differential equations, obtainable by a change of variables, in which the dynamics are particularly simple to understand [28]. We talk more about normal forms for Hamiltonian systems in section 3.3.

In Hamiltonian systems, it is well-known (Williamson’s theorem) that if λ is an eigenvalue, then so are $-\lambda$, $\bar{\lambda}$, and $-\bar{\lambda}$. This implies that the eigenvalues can occur in four types of groupings, up to multiplicity: complex quadruplets (Krein quartets) $\{\lambda, \bar{\lambda}, -\lambda, -\bar{\lambda}\}$ with nonzero real and imaginary parts, real-valued pairs $\{\lambda, -\lambda\}$, purely imaginary pairs $\{i\mu, -i\mu\}$ and zero eigenvalues of even algebraic multiplicity.

The symmetry-breaking, or Hamiltonian pitchfork, bifurcation occurs when, as a parameter is varied, a purely imaginary pair of eigenvalues collide at the origin, producing a purely real pair. Here, small perturbations to the origin initially grow monotonically due to the real positive eigenvalue. See figure 2(a) and (b). At the bifurcation point, the spectrum contains a zero of multiplicity-two.

A solution may also lose stability when, as the parameters are varied, two pairs of pure imaginary eigenvalues collide at a nonzero point on the imaginary axis, and the four eigenvalues recombine to form a quartet of fully complex eigenvalues. The linear stability is determined by the form of H_2 while the dynamics in a neighborhood of the equilibrium also depends on the higher-order terms. There are several different normal forms for a pair of complex conjugate double eigenvalues

$$H_{1;\pm 1}^{\text{SS}} = (\Omega + \delta_1) |z_1|^2 + (\pm\Omega + \delta_2) |z_2|^2. \tag{2.8}$$

At $\delta_1 = \delta_2 = 0$, these systems are possess the semisimple 1 : 1 or semisimple 1 : -1 resonance, depending on the \pm sign, because the frequencies of $J\nabla H_2$ at $\delta_1 = \delta_2 = 0$ are

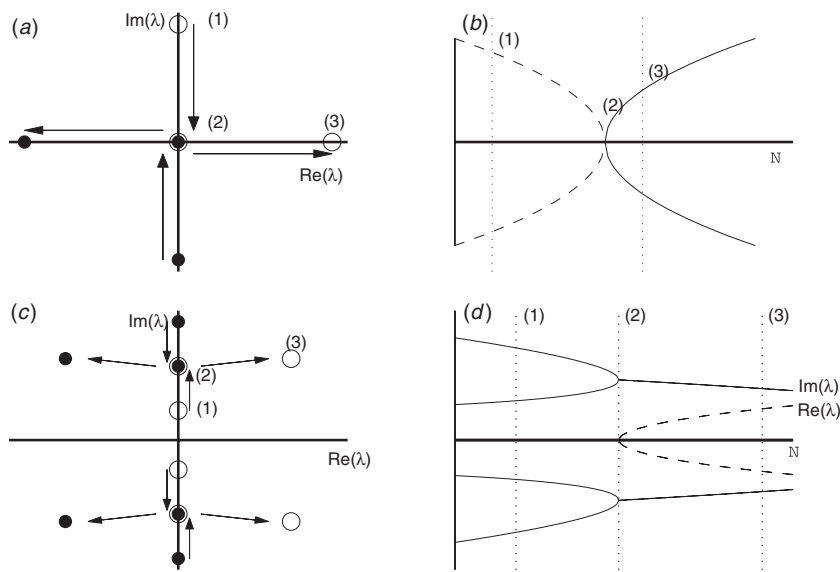


Figure 2. (a) The path of the eigenvalues as a parameter is varied in the Hamiltonian pitchfork bifurcation. (b) The real and imaginary parts of the eigenvalues. (c) The path of the eigenvalues as an parameter is varied, resulting in a Krein collision. (d) The real and imaginary parts of the eigenvalues. After Luzzatto–Fegiz and Williamson [36].

in ratios $1 : \pm 1$, and satisfy resonance relations of the form (2.7) with $k = (1, \mp 1)$. In both of these cases, the matrix JK is semisimple (diagonalizable over \mathbb{C}). We may refer to the bifurcations in these two systems, depending on the \pm sign, as the semi-simple positive-definite (SPHH) and the semisimple indefinite (SIHH) Hamiltonian Hopf bifurcations.

The third normal form that possesses a pair of multiplicity-two eigenvalues on the imaginary axis occurs when the matrix JK is non-semisimple, i.e. has nontrivial Jordan form. This normal form is referred to in the geometric mechanics literature as the Hamiltonian Hopf (HH) bifurcation, while in the nonlinear waves literature, the HH label has been applied to any of the three normal forms. The failure to recognize this distinction has caused a lot of confusion in the nonlinear waves literature, and results applicable to the Hamiltonian Hopf bifurcation have often been inappropriately cited in reference to systems with either of the two semisimple normal forms. There exists a very small literature studying the two semisimple cases, notably [21] and [33], while a wealth of papers examine the HH bifurcation, for example [20, 22, 23].

The system under study here undergoes the SIHH bifurcation. Nonetheless, we will use the abbreviation HH in this paper, as is familiar, and the abbreviation SIHH is awkward.

Readers unfamiliar with the Hamiltonian context may nonetheless be aware that the generic (non-Hamiltonian) Hopf bifurcation may be classified as supercritical or subcritical. This classification depends on the *nonlinear* terms in the equations, whereas the classification given above depends solely on the linear part. A similar classification is made by Lahiri and Roy for the nonsemisimple HH bifurcation using formal averaging of a different type than given here [34].

They find two types of bifurcations, depending on certain coefficients in the cubic and quartic terms in the Hamiltonian. In their *Type I* bifurcation, they find that there exists a critical

nonlinearity coefficient $\mathcal{N}_{\text{crit}} > 0$. For $\mathcal{N} > \mathcal{N}_{\text{crit}}$, the averaged equations possess a periodic orbit a distance $d \propto \sqrt{\mathcal{N} - \mathcal{N}_{\text{crit}}}$ from the origin, regardless of whether the nonlinear terms are subcritical or supercritical. In their *Type II* bifurcation, there exists no nonzero periodic orbit near zero on the unstable side of the bifurcation. Johansson makes a similar observation in his study of the NLS trimer [11] but does not comment on the difference between the semisimple and non-semisimple bifurcations—in fact, a straightforward computation shows the bifurcation for the trimer is semisimple, so the results of Lahiri and Roy do not apply. The analysis of Chow and Kim [33] serves a similar purpose for the SIHH bifurcation, but the dynamics are too varied to fit into a simple dichotomy.

2.4.4. Krein Signatures. Whether the collision of eigenvalues on the imaginary axis leads to instability is determined by the *Krein signatures* [35] associated with them. Let I_ω be the eigenspace corresponding to the eigenvalues $\pm i\omega$, with basis $\{\xi_1, \dots, \xi_{2m}\}$. Defining $K^{(\omega)}$ to be the restriction of K to I_ω , which can be constructed explicitly, using (complex) inner products to define a matrix

$$K_{j,k}^{(\omega)} = \langle \xi_j, K\xi_k \rangle.$$

Since $K^{(\omega)}$ is self-adjoint, we can define the positive (respectively, negative) Krein signature of I_ω to be the number of positive (resp., negative) eigenvalues of $K^{(\omega)}$.¹ An important theorem on stability [35] states that if I_ω has mixed signature, i.e. if both its positive and negative signatures are nonzero, then upon perturbation the eigenvalues may split into a Krein quartet, and that this cannot happen if I_ω has purely positive (or purely negative) signature. As a consequence, when two pairs of purely imaginary eigenvalues of opposite Krein signature collide, they generically split into a Krein quartet, indicating that the origin has become unstable, with oscillatory dynamics due to their nonzero imaginary parts as sketched in figure 2(c) and (d).

3. The finite-dimensional model

3.1. Derivation of the model

We decompose the solution to equation (2.3) as the following time-dependent linear combination:

$$u = c_1(t)U_1(x) + c_2(t)U_2(x) + c_3(t)U_3(x) + \eta(x; t), \quad (3.1)$$

where the eigenfunctions U_j , defined in equation (2.1), are orthonormal and, for all t , $\eta(x; t)$ is orthogonal to the discrete eigenspace, i.e.

$$\langle U_i, U_j \rangle = \delta_{i,j} \quad \text{and} \quad \langle \eta(\cdot, t), U_j \rangle = 0, \quad \text{for } i, j = 1, 2, 3.$$

We define the projection operators on to the discrete eigenmodes

$$\Pi_j \zeta = \langle U_j, \zeta \rangle U_j \quad \text{for } j = 1, 2, 3, \quad (3.2)$$

and onto the continuous spectrum

$$\Pi_C \zeta = \zeta - (\Pi_1 + \Pi_2 + \Pi_3)\zeta.$$

¹ Mackay [35] provides a complete definition, which is also well defined for the cases of real eigenvalues and complex quartets as well as purely imaginary eigenvalues.

Substituting the decomposition (3.1) into NLS/GP (2.3) and applying these four projection operators gives evolution equations for the components of the decomposition. The following system of equations is equivalent to (2.3) under the assumptions of section 2.2:

$$\begin{aligned}
i \frac{dc_1}{dt} - \Omega_1 c_1 + \mathcal{N} [a_{1111} |c_1|^2 c_1 + a_{1113} (c_1^2 \bar{c}_3 + 2|c_1|^2 c_3) + a_{1122} (2c_1 |c_2|^2 + \bar{c}_1 c_2^2) \\
+ a_{1133} (2c_1 |c_3|^2 + \bar{c}_1 c_3^2) + a_{1223} (c_2^2 \bar{c}_3 + 2|c_2|^2 c_3) \\
+ a_{1333} |c_3|^2 c_3] = R_1(c_1, c_2, c_3, \eta); \\
i \frac{dc_2}{dt} - \Omega_2 c_2 + \mathcal{N} [a_{1122} (c_1^2 \bar{c}_2 + 2|c_1|^2 c_2) + 2a_{1223} (c_1 c_2 \bar{c}_3 + c_1 \bar{c}_2 c_3 + \bar{c}_1 c_2 c_3) \\
+ a_{2222} |c_2|^2 c_2 + a_{2233} (2c_2 |c_3|^2 + \bar{c}_2 c_3^2)] = R_2(c_1, c_2, c_3, \eta); \\
i \frac{dc_3}{dt} - \Omega_3 c_3 + \mathcal{N} [a_{1113} |c_1|^2 c_1 + a_{1133} (c_1^2 \bar{c}_3 + 2|c_1|^2 c_3) + a_{1223} (2c_1 |c_2|^2 + \bar{c}_1 c_2^2) \\
+ a_{1333} (2c_1 |c_3|^2 + \bar{c}_1 c_3^2) + a_{2233} (c_2^2 \bar{c}_3 + 2|c_2|^2 c_3) \\
+ a_{3333} |c_3|^2 c_3] = R_3(c_1, c_2, c_3, \eta); \\
i \partial_t \eta - H \eta + \mathcal{N} |\eta|^2 \eta = R_C(c_1, c_2, c_3, \eta), \tag{3.3}
\end{aligned}$$

where

$$a_{jklm} = \langle u_j, u_k u_l u_m \rangle$$

and we have used the invariance of the coefficients a_{jklm} under permutation of the four indices and the fact that $a_{jklm} = 0$ if $(j+k+l+m)$ is odd. The parameters are calculated numerically as needed for the numerical simulations. The remainder terms R_j are the projections of the remaining nonlinear terms of (2.3) onto the discrete eigenfunctions:

$$R_j = -\mathcal{N} \cdot \Pi_j F,$$

where Π_j is given in equation (3.2) and

$$\begin{aligned}
F = |c_1 U_1 + c_2 U_2 + c_3 U_3 + \eta|^2 (c_1 U_1 + c_2 U_2 + c_3 U_3 + \eta) \\
- |c_1 U_1 + c_2 U_2 + c_3 U_3|^2 (c_1 U_1 + c_2 U_2 + c_3 U_3).
\end{aligned}$$

The remainder term in the continuum portion is

$$R_C = -\mathcal{N} \cdot \Pi_C G,$$

where

$$G = |c_1 U_1 + c_2 U_2 + c_3 U_3 + \eta|^2 (c_1 U_1 + c_2 U_2 + c_3 U_3 + \eta) - |\eta|^2 \eta.$$

Ignoring the contributions of $\eta(x; t)$ to the solution yields a finite-dimensional approximation to (3.3); the reasoning for the change of notation $\mathcal{N} \rightarrow N$ is described afterward:

$$\begin{aligned}
i \frac{dc_1}{dt} - \Omega_1 c_1 + N [a_{1111} |c_1|^2 c_1 + a_{1113} (c_1^2 \bar{c}_3 + 2|c_1|^2 c_3) + a_{1122} (2c_1 |c_2|^2 + \bar{c}_1 c_2^2) \\
+ a_{1133} (2c_1 |c_3|^2 + \bar{c}_1 c_3^2) + a_{1223} (c_2^2 \bar{c}_3 + 2|c_2|^2 c_3) + a_{1333} |c_3|^2 c_3] = 0 \\
i \frac{dc_2}{dt} - \Omega_2 c_2 + N [a_{1122} (c_1^2 \bar{c}_2 + 2|c_1|^2 c_2) + 2a_{1223} (c_1 c_2 \bar{c}_3 + c_1 \bar{c}_2 c_3 + \bar{c}_1 c_2 c_3) \\
+ a_{2222} |c_2|^2 c_2 + a_{2233} (2c_2 |c_3|^2 + \bar{c}_2 c_3^2)] = 0 \\
i \frac{dc_3}{dt} - \Omega_3 c_3 + N [a_{1113} |c_1|^2 c_1 + a_{1133} (c_1^2 \bar{c}_3 + 2|c_1|^2 c_3) + a_{1223} (2c_1 |c_2|^2 + \bar{c}_1 c_2^2) \\
+ a_{1333} (2c_1 |c_3|^2 + \bar{c}_1 c_3^2) + a_{2233} (c_2^2 \bar{c}_3 + 2|c_2|^2 c_3) + a_{3333} |c_3|^2 c_3] = 0. \tag{3.4}
\end{aligned}$$

We have introduced the following slight change of notation in this equation. As system (3.3) is equivalent to equation (2.3), it conserves the L^2 norm

$$|c_1|^2 + |c_2|^2 + |c_3|^2 + \|\eta\|_2^2 = 1.$$

This implies that $|c_1|^2 + |c_2|^2 + |c_3|^2 \leq 1$, while system (3.4) possesses a finite-dimensional conserved quantity corresponding to the photon number of system (1.1),

$$|c_1|^2 + |c_2|^2 + |c_3|^2 = 1. \quad (3.5)$$

The conserved quantities in systems (2.3) and (3.4) are not equivalent, since the contribution of $\eta(x, t)$ is ignored in the latter. Recall that \mathcal{N} represents the total intensity and the sign of the nonlinearity in equation (1.1). Since the meaning of \mathcal{N} is slightly changed from equation (2.3) to system (3.4), we introduce the new constant N .

The above reduction demands some justification, either numerical or rigorous. One check is whether a numerically computed solution to (1.1) whose initial condition consists of a linear superposition of the eigenmodes stays close to the manifold $\eta(x, t) = 0$ for long times. Our PDE simulations, which are described in section 5.2 were run over long times, up to 20 000 oscillations of the phase $\theta(t)$. Although they were run with absorbing boundary conditions, the computed L^2 norm of the solution was in all cases conserved to within half of a percent, and the L^2 norm of the projection onto the three eigenfunctions conserved to within 0.6 percent. Further, figure 6 shows good qualitative agreement, and for shorter times quantitative agreement, between solutions to (1.1) and the approximation (3.4).

To rigorously justify the above assumptions is, of course, a significant task, and one which we delay to a subsequent paper. It should proceed in largely the same way as recent results. Here we discuss those results and in what sense those results justify the finite-dimensional truncation. Kirr *et al* [4] prove using a Lyapunov–Schmidt argument that standing waves given as the continuations of the linear eigenfunctions are well-approximated by solutions to the finite dimensional system, and that the critical amplitude at which such solutions lose stability in symmetry-breaking bifurcations is asymptotically close to the bifurcation value for the finite-dimensional problem. Marzuola and Weinstein [6] prove a shadowing theorem, in which certain quasiperiodic solutions to the finite-dimensional system are shadowed by solutions to NLS/GP (1.1) over long but finite times using an infinite-dimensional Floquet argument. This approach required the use of Strichartz estimates, and we should be able to prove similar theorems regarding periodic and quasiperiodic solutions in the present case. Pelinovsky and Phan [7] use a normal form argument that proves the results of Kirr without Lyapunov–Schmidt, and obtains short-time shadowing theorems like Marzuola for arbitrary small initial conditions, not just certain periodic orbits, without the need for Floquet analysis and using much simpler inequalities, at the cost of the estimates being valid on significantly shorter timescales. Of course, since the numerics below suggest that both the PDE and ODE evolve chaotically, such a shadowing theorem may have to be replaced by a much weaker statement. The proofs given in the above references depend on stricter assumption than those given in (S1)–(V3), particularly inequalities involving the coefficients a_{ijkl} .

3.2. Model reduction via symmetry

To understand the dynamics of system (3.4), it is useful to use the invariance of H under $c_j \rightarrow e^{i\alpha} c_j$ to reduce the number of degrees of freedom from three to two. This reduction is based on the Hamiltonian form

$$\begin{aligned}
 H = & \Omega_1|c_1|^2 + \Omega_2|c_2|^2 + \Omega_3|c_3|^2 - N\left[\frac{1}{2}a_{1111}|c_1|^4 + a_{1113}|c_1|^2(c_1\bar{c}_3 + \bar{c}_1c_3)\right. \\
 & + a_{1122}\left(\frac{1}{2}c_1^2\bar{c}_2^2 + 2|c_1|^2|c_2|^2 + \frac{1}{2}\bar{c}_1^2c_2^2\right) + a_{1133}\left(\frac{1}{2}c_1^2\bar{c}_3^2 + 2|c_1|^2|c_3|^2 + \frac{1}{2}\bar{c}_1^2c_3^2\right) \\
 & + a_{1223}\left(2|c_2|^2(c_1\bar{c}_3 + \bar{c}_1c_3) + c_1\bar{c}_2^2c_3 + \bar{c}_1c_2^2\bar{c}_3\right) + a_{1333}|c_3|^2(c_1\bar{c}_3 + \bar{c}_1c_3) \\
 & \left. + \frac{1}{2}a_{2222}|c_2|^4 + a_{2233}\left(\frac{1}{2}c_2^2\bar{c}_3^2 + 2|c_2|^2|c_3|^2 + \frac{1}{2}\bar{c}_2^2c_3^2\right) + \frac{1}{2}a_{3333}|c_3|^4\right] \quad (3.6)
 \end{aligned}$$

with evolution equations

$$i\dot{c}_j = \frac{\partial H}{\partial \bar{c}_j}; \quad j = 1, 2, 3. \quad (3.7)$$

We simplify the equations using generalized action-angle coordinates

$$c_1(t) = \sigma_1(t) e^{i\theta(t)}; \quad c_2(t) = \rho(t) e^{i\theta(t)}; \quad c_3(t) = \sigma_3(t) e^{i\theta(t)}, \quad (3.8)$$

where $\rho(t), \theta(t) \in \mathbb{R}$. ODEs for these variables are determined by inserting (3.8) into equations (3.6) and (3.7). The c_2 equation determines the evolution of $\theta(t)$ in terms of σ_1 and σ_3

$$\begin{aligned}
 \dot{\theta}(t) = & -\Omega_2 + N\left[a_{2222}(1 - |\sigma_1|^2 - |\sigma_3|^2) + \frac{1}{2}a_{1122}(\sigma_1^2 + 4|\sigma_1|^2 + \bar{\sigma}_1^2)\right. \\
 & \left. + a_{1223}(2\bar{\sigma}_3\sigma_1 + 2\bar{\sigma}_1\sigma_3 + \bar{\sigma}_1\bar{\sigma}_3 + \sigma_1\sigma_3) + \frac{1}{2}a_{2233}(\sigma_3^2 + 4|\sigma_3|^2 + \bar{\sigma}_3^2)\right]. \quad (3.9)
 \end{aligned}$$

This equation and the conservation law (3.5) are used to eliminate θ and ρ from the evolution equations for $\sigma_1(t)$ and $\sigma_3(t)$. These are integrated to give a reduced Hamiltonian depending solely on N, σ_1, σ_3 , and their complex conjugates:

$$\begin{aligned}
 H_R = & (-W + \epsilon)|\sigma_1|^2 + (W + \epsilon)|\sigma_3|^2 - N\left[\frac{1}{2}a_{1111}|\sigma_1|^4 + a_{1113}|\sigma_1|^2(\sigma_1\bar{\sigma}_3 + \bar{\sigma}_1\sigma_3)\right. \\
 & + \frac{1}{2}a_{1122}(1 - |\sigma_1|^2 - |\sigma_3|^2)(\sigma_1^2 + 4|\sigma_1|^2 + \bar{\sigma}_1^2) \\
 & + a_{1133}\left(\frac{1}{2}\sigma_1^2\bar{\sigma}_3^2 + 2|\sigma_1|^2|\sigma_3|^2 + \frac{1}{2}\bar{\sigma}_1^2\sigma_3^2\right) \\
 & + a_{1223}(1 - |\sigma_1|^2 - |\sigma_3|^2)(\sigma_1\sigma_3 + 2\sigma_1\bar{\sigma}_3 + 2\bar{\sigma}_1\sigma_3 + \bar{\sigma}_1\bar{\sigma}_3) \\
 & + a_{1333}|\sigma_3|^2(\sigma_1\bar{\sigma}_3 + \bar{\sigma}_1\sigma_3) \\
 & + \frac{1}{2}a_{2222}(1 - |\sigma_1|^2 - |\sigma_3|^2)^2 + \frac{1}{2}a_{2233}(1 - |\sigma_1|^2 - |\sigma_3|^2)(\sigma_3^2 + 4|\sigma_3|^2 + \bar{\sigma}_3^2) \\
 & \left. + \frac{1}{2}a_{3333}|\sigma_3|^4\right]. \quad (3.10)
 \end{aligned}$$

The term $c_2(t)$ may be recovered using the conservation law (3.5) to obtain $\rho(t)$ and equation (3.9) for $\theta(t)$.

Remark 4. This reduction involves defining a reference phase $\theta(t)$ and thus leads to reduced equations that are not equivariant with respect to rotation by a phase.

3.3. Averaging and further reduction of the ODE

We further reduce the system using averaging methods. This puts the equations into normal form, which identifies which terms in H_R have a significant effect on the dynamics at leading order. We formally apply the von Zeipel procedure, which applies when there is a resonance between eigenvalues [28, 37]. The averaged equations preserve some but not all features of the full system of equations—for example, hyperbolic equilibria and their local un/stable manifolds are preserved, but homoclinic orbits are not. The averaged system $\mathcal{H}_{\text{average}}$, equation (3.19), is completely integrable, but we do not expect general Hamiltonians, such as (3.10), to be. Our numerical computations, typified by figure 6, suggest that the full system is chaotic and thus not integrable.

To put the system in the correct form for averaging, we make two exact changes of variables. After using definition (4.4), and replacing ϵ in equation (2.2) by

$$\epsilon \rightarrow \mathfrak{s}\epsilon$$

with $\epsilon \geq 0$ and $\mathfrak{s} = \pm 1$, we first make the change of variables to canonical polar coordinates

$$\sigma_j \rightarrow \sqrt{\rho_j} e^{i\theta_j}; \quad j = 1, 3,$$

yielding a Hamiltonian:

$$\begin{aligned} H_{\text{polar}} = & W\rho_1 - W\rho_3 - \epsilon\mathfrak{s}(\rho_1 + \rho_3) + \epsilon v[(a_{1122} \cos 2\theta_1 + 2a_{1122} - a_{2222})\rho_1 \\ & + 2a_{1223}(2 \cos(\theta_1 - \theta_3) + \cos(\theta_1 + \theta_3))\sqrt{\rho_1}\sqrt{\rho_3} \\ & + (a_{2233} \cos 2\theta_3 - a_{2222} + 2a_{2233})\rho_3 \\ & + \frac{1}{2}(-2a_{1122} \cos 2\theta_1 + a_{1111} - 4a_{1122} + a_{2222})\rho_1^2 \\ & + 2((a_{1113} - 2a_{1223}) \cos(\theta_1 - \theta_3) - a_{1223} \cos(\theta_1 + \theta_3))\rho_1^{3/2}\rho_3^{1/2} \\ & - (a_{1122} \cos 2\theta_1 - a_{1133} \cos 2(\theta_1 - \theta_3) + a_{2233} \cos 2\theta_3 \\ & + 2a_{1122} - 2a_{1133} - a_{2222} + 2a_{2233})\rho_1\rho_3 \\ & - 2((2a_{1223} - a_{1333}) \cos(\theta_1 - \theta_3) + a_{1223} \cos(\theta_1 + \theta_3))\rho_1^{1/2}\rho_3^{3/2} \\ & + \frac{1}{2}(-2a_{2233} \cos 2\theta_3 + a_{2222} - 4a_{2233} + a_{3333})\rho_3^2]. \end{aligned} \quad (3.11)$$

Averaging methods allow one to simplify a system by replacing some or all of its oscillatory terms by their means, which is accomplished using a sequence of near-identity changes of variables. Leading-order linear terms that satisfy a resonance condition, as in (2.7), render some of these equations unsolvable due to zero denominators. Were it not for such resonances between the eigenvalues, one could formally remove all terms containing trigonometric functions and fractional powers of ρ_1 and ρ_3 , putting the system in the so-called Birkhoff normal form. In the present case, the leading order linear part $H_2 = W\rho_1 - W\rho_3$ is $1 : -1$ resonant (semisimple and indefinite), so the system cannot be completely averaged and the Gustavson normal form applies, in which all but the resonant terms are averaged away. For more information see Wiggins [28, section 19.10, section 20.9].

The canonical change of variables

$$\theta_1 = \phi_1, \quad \theta_3 = -\phi_1 + \phi_3, \quad \rho_1 = I_1 + I_3, \quad \rho_3 = I_3$$

puts the Hamiltonian into the form

$$H_{\text{reduced}}(\vec{I}, \vec{\phi}) = H_0(I_1) + \epsilon H_1(I_1, I_3, \phi_1, \phi_3), \quad (3.12)$$

where

$$H_0(I_1) = WI_1 \quad \text{and} \quad H_1 = H_1^{\text{mean}}(I_1, I_3) + H_1^{\text{osc}}(I_1, I_3, \phi_1, \phi_3)$$

and H_1^{osc} has period π in ϕ_1 and 2π in ϕ_3 . In general, the term H_0 may be written as the inner product

$$H_0 = \langle \omega, \vec{I} \rangle,$$

so that, in this case, $\omega = (W, 0)$. Equation (3.12) shows that ϕ_1 oscillates on an $O(1)$ time scale since $\frac{d}{dt}\phi_1 = W + O(\epsilon)$, while I_1, I_3 and ϕ_3 oscillate slowly, on an $O(\epsilon^{-1})$ time scale. For this reason ϕ_1 , but not ϕ_3 , can be averaged out.

In the present problem, H_1^{osc} contains five terms, details omitted:

$$\begin{aligned} H_1^{\text{osc}} = & \sum_{k \in K} H_1^k(I_1, I_3) \cos \langle k, \vec{\phi} \rangle; \\ K = & K_{\text{res}} \cup K_{\text{non}} = \{(0, 1)\} \cup \{(2, 0), (2, -1), (2, -2), (4, -2)\}. \end{aligned}$$

Applying definition (2.7) the ordered pair $(0, 1) \in K_{\text{res}}$ is resonant with ω , while the four in K_{non} are not.

The von Zeipel averaging procedure yields a partially averaged Hamiltonian as a formal power series in ϵ ,

$$I_j = \frac{\partial S}{\partial \phi_j}, \quad \psi_j = \frac{\partial S}{\partial J_j}, \quad (3.13)$$

$$S(J, \phi, \epsilon) = \langle \vec{J}, \vec{\phi} \rangle + \epsilon S_1(\vec{J}, \vec{\phi}) + \dots \quad (3.14)$$

$$\mathcal{H}(\vec{J}, \vec{\psi}) = \mathcal{H}_0(I) + \epsilon \mathcal{H}_1(\vec{J}, \vec{\psi}) + \dots \quad (3.15)$$

Equations of the form (3.13) generate a canonical near-identity change of variables $(I, \phi) \rightarrow (J, \psi)$ for any *generating function* $S(J, \phi)$, the downside being that S must be inverted in order to find J . A more modern approach using *Lie transforms* does not have this problem. Plugging the expansion for $I = S_\phi$ into the Hamiltonian (3.12), setting this equal to the series (3.15) for \mathcal{H} and equating orders of ϵ , one finds at $O(1)$, $\mathcal{H}_0 = H_0$, and at order ϵ ,

$$\mathcal{H}_1(J, \psi) = \langle \nabla_J H_0, \nabla_{\vec{\phi}} S_1 \rangle + H_1(\vec{J}, \vec{\psi}) = \langle \omega, \nabla_{\vec{\phi}} S_1 \rangle + H_1(\vec{J}, \vec{\psi}).$$

The terms in S_1 are chosen to eliminate the fast phases from H_1 . The method proceeds by eliminating terms in H_1 of the form $H_1^k \cos \langle k, \vec{\phi} \rangle$ one at a time by solving *homological equations* of the form

$$(\omega \cdot \nabla_{\vec{\phi}}) S_1^k + H_1^k \cos \langle k, \vec{\phi} \rangle = 0.$$

For $k \in K_{\text{res}}$, this equation is unsolvable, since $\cos \langle k, \vec{\phi} \rangle$ is in the nullspace of the operator $\omega \cdot \nabla_{\vec{\phi}}$. Terms involving $k \in K_{\text{non}}$ may be eliminated, so that

$$S_1 = \sum_{k \in K_{\text{non}}} \frac{-H_1^k}{\langle k, \omega \rangle} \sin \langle k, \vec{\phi} \rangle.$$

This transforms the Hamiltonian to

$$\mathcal{H}(\vec{J}, \vec{\psi}) = WJ_1 + \epsilon \mathcal{H}_1(J_1, J_3, \psi_3) + \epsilon^2 \mathcal{H}_{\text{remainder}}(J_1, J_3, \psi_1, \psi_3; \epsilon), \quad (3.16)$$

where

$$\begin{aligned} \mathcal{H}_1(J_1, J_3, \psi_3) &= \alpha_1 J_1 + \alpha_3 J_3 + \alpha_{1,1} J_1^2 + \alpha_{1,3} J_1 J_3 + \alpha_{3,3} J_3^2 \\ &+ 2_{1223} \nu (J_1 + 2J_3 - 1) \sqrt{J_3} \sqrt{J_3 + J_1} \cos \psi_3 \end{aligned} \quad (3.17)$$

and $\mathcal{H}_{\text{remainder}}$ is 2π -periodic in ψ_1 . We delay writing down the coefficients.

System (3.16) is in the proper form for the reduction procedure of [38, section 4.8]. We consider the dynamics on the level set $\mathcal{H} = hW$ and solve for J_1 in (3.17) as a series in ϵ . Such a solution exists when $\frac{\partial}{\partial J_1} \mathcal{H} \neq 0$, or equivalently when $\frac{d}{dt} \psi_1 \neq 0$. In this case ψ_1 is a time-like variable; the reduction then gives simplified equations for the evolution of (J_3, ψ_3) with respect to ψ_1 . The ansatz

$$J_1 = L(J_3, \psi_3; h) = J_1^{(0)} + \epsilon J_1^{(1)} + \dots$$

yields expansion

$$J_1^{(0)} = h; \quad J_1^{(1)} = -\frac{1}{W} \mathcal{H}_1(h, J_3, \psi_3)$$

and J_3 and ψ_3 evolve under the effective Hamiltonian

$$\mathcal{H}_{\text{reduced}}(J_3, \psi_3, \tau; h) = -L = -h + \frac{\epsilon}{W} \mathcal{H}_1(J_3, \psi_3; h) + \epsilon^2 \mathcal{H}_2(J_3, \psi_3, \tau; h). \quad (3.18)$$

Ignoring any terms independent of J_3 and ψ_3 that do not effect the dynamics

$$\mathcal{H}_1(J_3, \psi_3; h) = \gamma_1 J_3 + \gamma_2 J_3^2 + \gamma_3 \sqrt{J_3} \sqrt{J_3 + h} (2J_3 + h - 1) \cos \psi_3$$

with

$$\gamma_1 = 2s + (-a_{1111}h + 2a_{1122}(3h - 1) - 2a_{1133}h - 2a_{2222}(h - 1) + 2a_{2233}(h - 1)) \nu$$

$$\gamma_2 = \frac{\nu}{2} (-a_{1111} + 8a_{1122} - 4a_{1133} - 4a_{2222} + 8a_{2233} - a_{3333})$$

$$\gamma_3 = 2\nu a_{1223}.$$

Remark 5. The implicit function theorem will fail if there exists t_0 such that $\frac{d\psi_1}{dt} |_{t=t_0} = \frac{\partial \mathcal{H}}{\partial J_1} = 0$; if ψ_1 does not grow monotonically, it cannot be used as a proxy for time. Our simulations show this is the case, for example, in figure 6, row (d).

System (3.18) satisfies some easily verified smoothness requirements in order to apply the averaging theorem, as stated by Guckenheimer and Holmes [38, theorem 4.1.1]. The theorem guarantees that there exists a change of variables

$$J = J_3 + O(\epsilon), \quad \psi = \psi_3 + O(\epsilon)$$

such that the solution to the averaged system with Hamiltonian

$$\mathcal{H}_{\text{average}} = \frac{\epsilon}{W} \mathcal{H}_1(J, \psi; h) \tag{3.19}$$

agrees with solutions to system (3.18) with $O(\epsilon)$ error $O(\epsilon^{-1})$ timescales. Further, for sufficiently small ϵ , hyperbolic equilibria and their local invariant manifolds of system (3.19) correspond to hyperbolic periodic orbits and their local invariant manifolds of system (3.18). Similarly elliptic equilibria of (3.19) correspond to elliptic periodic solutions of (3.18).

By the conservation law (3.5), ρ_1 and ρ_3 in system (3.11) are confined to the triangle

$$0 \leq \rho_1 \leq 1; \quad 0 \leq \rho_3 \leq 1; \quad 0 \leq \rho_1 + \rho_3 \leq 1.$$

In system (3.18), this becomes a constraint on the conserved parameter h and the variable J ,

$$-1 \leq h \leq 1; \quad \max(-h, 0) \leq J \leq \frac{1-h}{2}$$

in the case $0 \leq h \leq 1$. In this case, the phase space is the disk $J \leq \frac{1-h}{2}$.

Due to the higher-order terms \mathcal{H}_2 in equation (3.18), the conservation of h is only approximate in system (3.18). Formally, one may perform a countable sequence of changes of variables that transform system (3.18) into completely integrable form. This corresponds to defining a change of variables as a power series in ϵ . Generally, this power series has radius of convergence zero, because the full system is not itself integrable, which we can see from the apparent chaotic dynamics in the numerical solution given in figure 6(c). This suggests that the solution 6(b) is also very weakly chaotic, but with a much smaller chaotic region and a longer chaotic timescale.

4. Stability and dynamics near the first excited state: analysis

Just as other studies have begun by focusing on the destabilization of the ground state of the two-well system via symmetry breaking [4, 6, 7], the goal of this paper is to understand the

dynamics in the neighborhood of an HH bifurcation. We therefore consider the stability of, and the dynamics near, the antisymmetric mode $U_2(x, N)$, the nonlinear continuation of the first excited state U_2 of equation (2.1). In the reduced system (3.10) this is just the dynamics in the neighborhood of the origin. Future work will include a more thorough description of the global phase space including all the relative equilibria and relative periodic orbits for small N .

4.1. Relative equilibria of the reduced hamiltonian

We first look for relative equilibria of system (3.10) of the form

$$\begin{pmatrix} \sigma_1(t) \\ \sigma_3(t) \end{pmatrix} = \begin{pmatrix} x \\ y \end{pmatrix} e^{-i\Omega t},$$

which correspond, ultimately, to standing wave solutions of equation (1.2). This calculation is well-covered by Kapitula *et al* [8] who demonstrate the existence of two types. The first families persist in the $N \rightarrow 0$ limit. These correspond to the nonlinear deformations of the eigenfunctions defined in equation (2.1). The other family of solutions arise due to saddle-node bifurcations. These bifurcations are shown to take place for $N \gg \epsilon$, whereas we demonstrate HH bifurcations for $N = O(\epsilon)$. It is simple to show [4, 8] that a solution to equation (1.2) with real potential $V(x)$ are up to a constant phase factor, a real-valued function, as are relative equilibria of system (3.10). Thus, without loss of generality, we look for stationary solutions of the form

$$\begin{aligned} (\Omega - \Omega_1 + \Omega_2 + 3a_{1122}N)x + 3a_{1223}Ny + N((a_{1111} - 3a_{1122})x^3 + 3(a_{1113} - a_{1223})x^2y \\ + 3(a_{1133} - a_{1122})xy^2 - (3a_{1223} - a_{1333})y^3) = 0 \\ 3a_{1223}Nx + (\Omega + \Omega_2 - \Omega_3 + 3a_{2233}N)y + N((a_{1113} - 3a_{1223})x^3 + 3(a_{1133} - a_{2233})x^2y \\ + 3(a_{1333} - a_{1223})xy^2 - (3a_{2233} - a_{3333})y^3) = 0 \end{aligned}$$

with $x^2 + y^2 \leq 1$ and $x, y \in \mathbb{R}$.

The simplest solution is

$$x = y = 0, \quad \Omega = \Omega_2 - a_{2222} \tag{4.1}$$

which corresponds to an antisymmetric standing wave solution to (1.2), the nonlinear deformation of the eigenpair (U_2, Ω_2) of equation (2.1). There are two other standing-wave solutions for small N . These satisfy $x^2 + y^2 = 1$, so we write $x = \cos \theta(N)$, $y = \sin \theta(N)$. Taylor expanding $\theta(N)$ and $\Omega(N)$ for small N yields two solutions, one with θ near zero, corresponding to the nonlinear deformation of the eigenfunction U_1 , and one with θ near $\pi/2$, corresponding to the continuation of the eigenfunction U_3 . For a complete enumeration of the relative equilibria of (1.2), see [8].

4.2. Linearization of PDE solutions

Letting (U, Ω) be a solution of system (2.4) and consider small time-dependent perturbations of the form

$$u(x, t) = (U(x) + r(x, t) + is(x, t))e^{-i\Omega t}.$$

Then, linearizing and letting

$$(r, s) = (R(x), S(x))e^{\lambda t}$$

yields the eigenvalue problem

$$\lambda \begin{pmatrix} R \\ S \end{pmatrix} = \begin{pmatrix} 0 & -(\Omega + \partial_x^2 - V(x) + \mathcal{N}U^2(x)) \\ \Omega + \partial_x^2 - V(x) + 3\mathcal{N}U^2(x) & \end{pmatrix} \begin{pmatrix} R \\ S \end{pmatrix}. \tag{4.2}$$

While future studies will concentrate on analysis of this system in its own right, here we are interested in comparing the results of numerical stability studies of this system with those found for the model ODE.

4.3. Linearization of ODE

First, we determine the linear stability of the solution (4.1), the trivial solution to system (3.10). By inserting the form

$$\begin{pmatrix} \sigma_1(t) \\ \sigma_3(t) \end{pmatrix} = \begin{pmatrix} r_1(t) + is_1(t) \\ r_3(t) + is_3(t) \end{pmatrix}$$

into system (3.10), the linearized equations become

$$\frac{d}{dt} \begin{pmatrix} r_1 \\ r_3 \\ s_1 \\ s_3 \end{pmatrix} = \begin{pmatrix} 0_2 & -M_- \\ M_+ & 0_2 \end{pmatrix} \begin{pmatrix} r_1 \\ r_3 \\ s_1 \\ s_3 \end{pmatrix} \equiv M(\epsilon, N)u, \quad (4.3)$$

where 0_2 is a 2×2 matrix of zeros,

$$M_{\pm} = \begin{pmatrix} W - \epsilon + (m_{\pm}a_{1122} - a_{2222})N & m_{\pm}a_{1223}N \\ m_{\pm}a_{1223}N & -W - \epsilon + (a_{2233} + m_{\pm}a_{2222})N \end{pmatrix},$$

and $m_{\pm} = 2 \pm 1$. The matrix $M(\epsilon, 0)$ has imaginary eigenvalues $\lambda_{1,2}^{\pm} = \pm i(\Omega_1 - \Omega_2) = \pm i(-W + \epsilon)$ and $\lambda_{3,2}^{\pm} = \pm i(\Omega_3 - \Omega_2) = \pm i(W + \epsilon)$. For all N , $M(\epsilon)$ is symplectic, i.e. $M = JK$ where K is symmetric and

$$J = \begin{pmatrix} 0_2 & -I \\ I & 0_2 \end{pmatrix} \quad \text{so that} \quad K = \begin{pmatrix} M_+ & 0_2 \\ 0_2 & M_- \end{pmatrix}.$$

4.4. Analytical criterion for ODE bifurcation

In this section, we compute an analytic condition for a Krein collision in system (3.10). The Krein signatures associated with the frequencies $\pm(\Omega_2 - \Omega_1)$ and $\pm(\Omega_2 - \Omega_3)$ in system (4.3) are $\mathcal{K}(\pm i(\Omega_1 - \Omega_2)) = \text{sign}(\Omega_1 - \Omega_2)$ and $\mathcal{K}(\pm i(\Omega_3 - \Omega_2)) = \text{sign}(\Omega_3 - \Omega_2)$, implying by assumption (S1), that their Krein signatures are opposite. Thus, their collision leads to instability. In fact, the Krein signature can be interpreted as the direction of phase rotation, and since Ω_2 lies between Ω_1 and Ω_3 , the Krein signatures can be determined without performing this calculation.

Krein collisions occurs at N for which $P(\lambda; N)$, the characteristic polynomial of $M(\epsilon, N)$, has multiple roots. As is generic for Hamiltonian systems, P contains only even powers of λ . Letting $q = \lambda^2$ defines a quadratic polynomial $p(q; N)$, which has a multiple root at N where its discriminant vanishes. Defining

$$v = N/\epsilon, \quad (4.4)$$

the discriminant is

$$\Pi(v) = \epsilon^2(d_4(\epsilon)v^4 + d_3(\epsilon)v^3 + d_2(\epsilon)v^2 + d_1(\epsilon)v + d_0(\epsilon)) = 0, \quad (4.5)$$

where

$$\begin{aligned}
 d_4 &= (3a_{1122} - 4a_{2222} + 3a_{2233})^2 (a_{1122}^2 - 2a_{2233}a_{1122} + 4a_{1223}^2 + a_{2233}^2) \epsilon^2 \\
 d_3 &= 8(a_{1122} - a_{2233})(a_{1122} - a_{2222} + a_{2233})(3a_{1122} - 4a_{2222} + 3a_{2233})W\epsilon \\
 &\quad - 8(3a_{1122} - 4a_{2222} + 3a_{2233})(a_{1122}^2 - 2a_{2233}a_{1122} + 4a_{1223}^2 + a_{2233}^2) \epsilon^2 \\
 d_2 &= 16(a_{1122} - a_{1223} - a_{2222} + a_{2233})(a_{1122} + a_{1223} - a_{2222} + a_{2233})W^2 \\
 &\quad - 8(a_{1122} - a_{2233})(7a_{1122} - 8a_{2222} + 7a_{2233})W\epsilon \\
 &\quad + 16(a_{1122}^2 - 2a_{2233}a_{1122} + 4a_{1223}^2 + a_{2233}^2) \epsilon^2 \\
 d_1 &= 32(a_{1122} - a_{2233})W\epsilon - 32(a_{1122} - a_{2222} + a_{2233})W^2 \\
 d_0 &= 16W^2.
 \end{aligned}$$

This is solved numerically or by a perturbation expansion $\nu = \nu_0 + O(\epsilon)$ which gives double eigenvalues at

$$N_{\text{KC},\pm} = \frac{\epsilon}{-a_{1122} \pm a_{1223} + a_{2222} - a_{2233}} + O(\epsilon^2). \tag{4.6}$$

Thus, there are Krein collisions for small values of ϵ , under the assumption that the denominator of this equation is bounded away from zero.

4.5. Dynamics of the averaged system \mathcal{H}_1

We are interested in the dynamics near the trivial solution of system (3.10), $(\sigma_1, \sigma_3) = (0, 0)$, which we showed in the previous section to destabilize via a semisimple implicit HH bifurcation.

This fixed point lies on the level set $h = 0$ in the truncated averaged system (3.19), so we can gain insight into the behavior of solutions to the system near this solution by looking at its phase space for $h = 0$. There is a slightly different structure for general h , which is the subject of ongoing investigation.

First, we define two invariant subspaces: Λ_{odd} is simply the origin in system (3.10), corresponding to all the energy in system (2.3) being in the mode $U_2(x)$. In the reduced system (3.19), this invariant set only intersects the set $h = 0$ where it corresponds to the left boundary $J = 0$. The second subspace is

$$\Lambda_{\text{even}} = \{(\sigma_1, \sigma_3) \mid |\sigma_1|^2 + |\sigma_3|^2 = 1\}$$

corresponding to the case where all the energy in system (2.3) is in the two modes with even symmetry. In the averaged system (3.19), Λ_{even} is simply the right boundary $J = \frac{1-h}{2}$.

On the set $h = 0$, the level set of system (3.19) corresponding to the origin in $(z_1, z_3, \bar{z}_1, \bar{z}_3)$ -space is

$$\begin{aligned}
 \mathcal{S}_0 &= \{(J, \psi) \mid \gamma_1 J + \gamma_2 J^2 + \gamma_3 (2J^2 - J) \cos \psi = 0\} \\
 &= \Lambda_{\text{odd}} \cup \left\{ (J, \psi) \mid \cos \psi = \frac{\gamma_1 + \gamma_2 J}{\gamma_3 (1 - 2J)} \right\}.
 \end{aligned}$$

There exist fixed points on Λ_{odd} if the second set contains points with $J = 0$. At these points,

$$\cos \psi = \frac{\gamma_1}{\gamma_3} = -\frac{(a_{1122} - a_{2222} + a_{2233})\nu - \mathfrak{s}}{a_{1223}\nu}. \tag{4.7}$$

These solutions exist if $|\gamma_1/\gamma_3| \leq 1$ and there exist bifurcations when the right-hand side is ± 1 , i.e. at

$$\nu_{\text{KC}} = \frac{\mathfrak{s}}{\pm a_{1223} + a_{1122} - a_{2222} + a_{2233}},$$

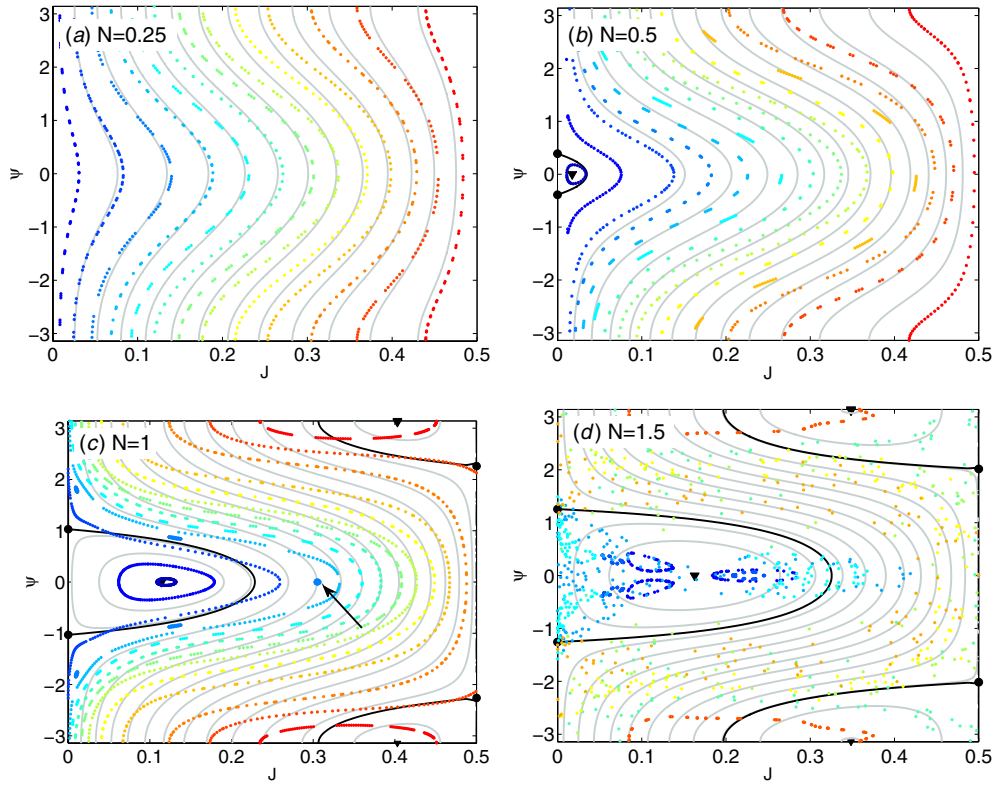


Figure 3. Gray lines: level sets of $\mathcal{H}1$. Black lines: heteroclinic orbits. Heteroclinic orbit and fixed point J_{NO} toward left appears for $N > 0.445$; heteroclinic orbit and fixed point J_{NE} to right for $N > 0.530$. Scattered points are Poincaré section $\psi_1 = 0$ of simulations of system (3.10); see section 5.2.

which recapitulates the Krein collision condition (4.6). For $\nu < \nu_{KC}$, the dynamics is described by monotonically decreasing angle ψ (determined from the sign of the numerically calculated γ_1) and small oscillations in the amplitude J ; see the gray lines in figure 3(a).

For $\nu > \nu_{KC}$, the two hyperbolic fixed points on Λ_{odd} are connected by three heteroclinic orbits: two on Λ_{odd} and one with $J > 0$. These separatrices enclose a region of phase space in which the solutions lie on closed curves with (J, ψ) oscillating about a nonlinear center with $\sin \psi = 0$ and

$$J = J_{NO} \equiv \frac{2(a_{1122} \pm a_{1223} - a_{2222} + a_{2233} - \mathfrak{s}/\nu)}{-a_{1111} - 8a_{1122} - 4a_{1133} \pm 4a_{1223} + 4a_{2222} - 8a_{2233} + a_{3333}}. \quad (4.8)$$

The subscript NO stands for nearly-odd, since this solution bifurcates from Λ_{odd} ; see figure 3(b). Whether this equilibrium lies on $\psi = 0$ or $\psi = \pi$ is determined by whether J_{NO} solves equation (4.7) with $\cos \psi = 1$ or -1 . In the computations we have performed $\psi = 0$ has occurred for $\mathfrak{s} < 0$ and $\psi = \pi$ for $\mathfrak{s} > 0$.

4.5. *Additional structure from the averaged system.* A similar bifurcation exists involving Λ_{even} . Two hyperbolic equilibria on Λ_{even} exist at

$$J = \frac{1}{2}; \quad \cos \psi_F = \frac{-\gamma_1 - \gamma_2}{\gamma_3}. \quad (4.9)$$

These exist only if the right hand side has magnitude less than one which gives a necessary condition on the amplitude $\nu \geq \nu_F$ for their existence, where

$$\nu_F = \frac{5}{\frac{1}{4}a_{11111} - a_{1122} + a_{1133} \mp a_{1223} - a_{2233} + \frac{1}{4}a_{33333}}. \quad (4.10)$$

The dynamics of the averaged system near this structure are exactly analogous to the dynamics near Λ_{odd} described above. For $\nu > \nu_F$, equation (4.9), the two saddles are connected by three heteroclinic orbits, two of them contained in Λ_{even} and a third one surrounding an additional elliptic equilibrium with $J = J_{NE}$ (nearly even) and $\psi = \pi$ or $\psi = 0$; see figure 3(c).

Remark 6. For $h \neq 0$, the structure near Λ_{even} persists: there is a critical amplitude $\nu_F(h)$ which approaches ν_F as $h \rightarrow 0$, and for $\nu > \nu_F(h)$, there exist three fixed points and three heteroclinic orbits. Near Λ_{odd} , the behavior is somewhat different as will be explained further in an upcoming article. These differences do not effect the claims made here.

Note that the equilibria of system (3.19) found in this section correspond to periodic orbits of equation (3.10) and are not solutions to system (2.4). The averaged system (3.19) is valid for small values of ϵ and describes the dynamics for small $|N|$ demonstrated numerically in figure 5. More concretely, the averaged system possesses the bifurcations described by equation (4.6), but not the other two roots of equation (4.5) that may exist for $N = O(1)$.

The evolution in the averaged system shown in figure 3 appears very similar to that in [6, figure 8] for a two-well defect. The separatrix that bifurcates from Λ_{odd} is a close analog of the homoclinic origin to the origin in the Hamiltonian pitchfork bifurcation. The equilibria and separatrix that bifurcate from Λ_{even} have no analog in their model. The behavior of solutions to (3.10) closely follows that of the averaged system for small ν but demonstrates torus break-up and chaos for larger values of ν , as discussed in section 5.2. This is qualitatively different from Marzuola and Weinstein, because the system they study is integrable.

5. Stability and dynamics near the first excited state: numerical simulations

In all computations and simulations below, we use the potential depicted in figure 1 with frequencies $\{-11.1, -10, -9.1\}$.

5.1. Bifurcation study: spectrum of linearization

We first consider for what values of ϵ equation (4.6) provides a good approximation to the critical value N_{KC} when the eigenvalues satisfy assumption (2.2). We show an example in figure 4. The potential pictured in figure 1 corresponds to choosing $\epsilon = -0.1$, and the potential's shape does not change much as ϵ is varied. This figure shows that for small values of ϵ the system has Krein collisions at both positive and negative values of N , but that for larger values of ϵ these collisions may cease to exist for large W . This change in character occurs for values of ϵ where two roots of the discriminant (4.5) collide and annihilate each other, i.e. where the *discriminant of the discriminant* $\Pi(N)$ vanishes. Next we compare the bifurcation structure of ODE system (3.10) with that of standing waves of system (1.2). We convert equation (2.4) to an algebraic equation using a pseudospectral approximation for the

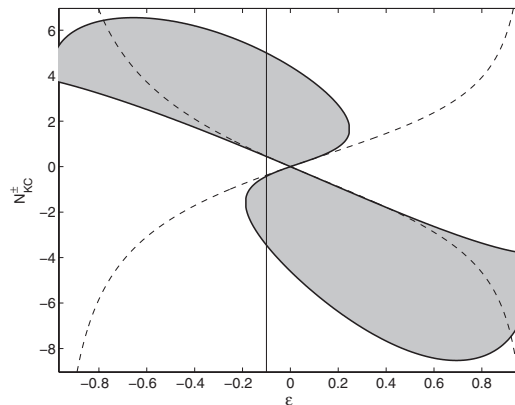


Figure 4. Stability diagram. Shaded areas: stability domains in (ϵ, N) space for the trivial solution. Solid lines: locations of Krein collisions. Dashed line: approximate Krein collision curves given by (4.6). The potential is defined by $\Omega_2 = -10$ with $W = 1$ and varying ϵ .

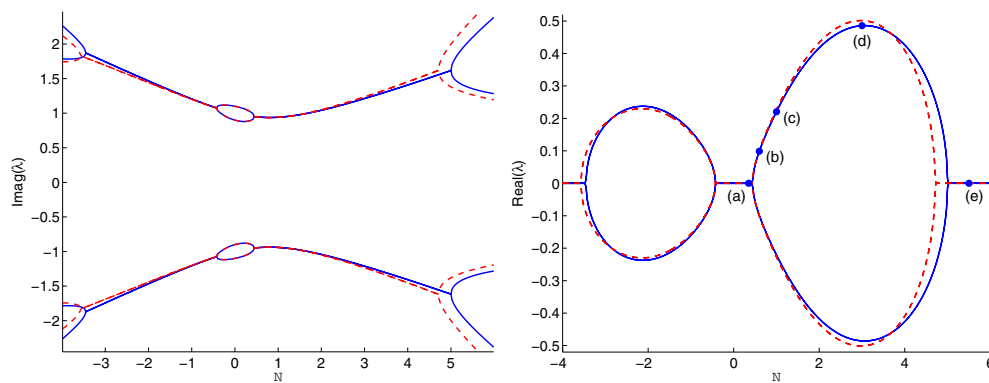


Figure 5. The imaginary and real parts of the discrete eigenvalues of the reduced ODE (solid) PDE standing wave (dashed). Both show four HH bifurcations, the PDE at $N \in \{-3.58, -0.44, 0.44, 4.71\}$, and the ODE at $N \in \{-3.46, -0.44, 0.44, 5.01\}$.

derivative, which we solve using Matlab’s `fsolve` command. We then calculate Σ_{PDE} , the discrete spectrum of the linearized PDE (4.2), using a pseudospectral approximation. We compare this with the Σ_{ODE} , spectrum of the matrix $M(\epsilon, N)$ in equation (4.3). Figure 5 shows excellent agreement between Σ_{PDE} and Σ_{ODE} , even for large N .

5.2. ODE and PDE dynamics

In this section we compare numerical simulations of ODE system (3.10) with those of the nonlinear Schrödinger equation (2.3).

We simulate the (σ_1, σ_3) system (3.10) using the Hamiltonian Boundary Value Method of Brugnano *et al* [39], a symplectic method that exactly conserves the energy in polynomial Hamiltonian systems. To compare these numerical solutions to the phase portraits of the averaged system (3.19), we follow the sequence of changes of variables in section 3.3 to transform the variables into the action-angle coordinates (J, ψ) in equation (3.16). We then

compute Poincaré sections of (J_3, ψ_3) on the section $\psi_1 \equiv 0 \pmod{2\pi}$, which are compared with the phase portraits of the system (3.19) in figure 3. For small values of N , the Poincaré sections resemble the level sets of the averaged system, with the agreement decreasing for larger N , parts (a) and (b). As N is increased and new families of periodic orbits appear in the averaged system, we find Poincaré sections lying near tori with the same topology, parts (b)–(d). For larger N , the non-integrability of system (3.10) becomes apparent. We show in subfigure (c), marked with an arrow, one resonant torus that has broken up into an island chain with five islands. In subfigure (d), the Poincaré sections no longer follow the trajectories of system (3.10) well at all.

We next present simulations that demonstrate the dynamics of small perturbations to the antisymmetric standing wave $u_2^N(x)$ defined in section 1.2, and to compare these solutions of NLS/GP (2.3) with approximations constructed from solutions to the (σ_1, σ_3) system (3.10). To simulate solutions to (2.3), we use a Matlab code written by T Dohnal. It uses fourth-order centered differences in space, and an implicit-explicit additive Runge–Kutta method for time stepping [40] and, most importantly for long-term simulation, uses perfectly matched layers (PML) to handle the outgoing radiation [41].

For the NLS simulations, we begin with the same values of σ_1 and σ_3 as above, and compute $\sigma_2 = \rho = (1 - \sigma_1^2 - \sigma_3^2)^{1/2}$. From these, we construct the initial conditions with $u(x, 0) = \sum_{j=1}^3 \sigma_j U_j(x)$. We then post-process these PDE simulations to compare them with ODE system (3.10). First we numerically compute the projections (3.2), giving parameters $c_j(t)$. Dividing c_j by the phase of $c_2(t)$ give values analogous to σ_j and $\rho(t)$. We then repeat the steps outlined above to obtain variables akin to (J_3, ψ_3) .

Numerical experiments for the five values of N marked in figure 5 are displayed in figure 6. In all cases the initial conditions used are $\sigma_1 = \sigma_3 = 10^{-5}$. The first column contains time series of $\Re\sigma_1$ for numerical solutions to (2.3) and (3.10). The second, a Poincaré section on $\psi_1 \equiv 0 \pmod{2\pi}$; plotted are $X = \sqrt{J_3} \cos \psi_3$ versus $Y = \sqrt{J_3} \sin \psi_3$ for simulations of the same two systems. The third column contains the amplitude $|u(x, t)|$, reconstructed from a numerical simulation of system (3.10), computed using (3.1) and (3.8). Column four contains $|u(x, t)|$ from direct numeral simulation of NLS/GP, equation (2.3).

In the five computations, we see that (a) for small $N < N_{KC}$, the solution stays in a neighborhood of zero and oscillates quasiperiodically. (b) For N slightly greater than N_{KC} , the solution undergoes a sequence of homoclinic bursts, where an oscillatory bright spot grows periodically in the middle well, taking energy from the two outer wells. (c) For somewhat larger N , the spacing between the bursts becomes irregular, and the Poincaré section displays a ‘lace curtain’ structure typical of Hamiltonian chaos, with very similar structure in the ODE and PDE simulations. (d) For N chosen to maximize the instability, the dynamics is very irregular and fills the energetically accessible region of phase space. The ODE and PDE simulations separate exponentially, but display remarkably similar dynamics. (e) For N sufficiently large, the trivial solution is again stable. In simulation (d), we are unable to use ψ_1 as a time-like variable as in (3.18) because it is non-monotonic; see remark 5. We instead display the Poincaré section $\sigma_1 \in \mathbb{R}$.

The equilibrium J_{NO} of the averaged equation exists for $N > N_{KC}$, corresponding to a periodic orbit of system (3.10). We solve for this periodic orbit numerically, which then can be used to construct a *relative* periodic orbit of system (3.4). Using the decomposition (3.1) with the assumption $\eta = 0$, we can approximate a quasiperiodic time-dependent field which should be shadowed by a solution to (1.1).

This reconstructed field, computed for the parameter value $N = 2$, is shown in figure 7. The bright spots move around due to constructive and destructive interference between the three eigenfunctions. The odd symmetry is broken, as the minimum amplitude location meanders

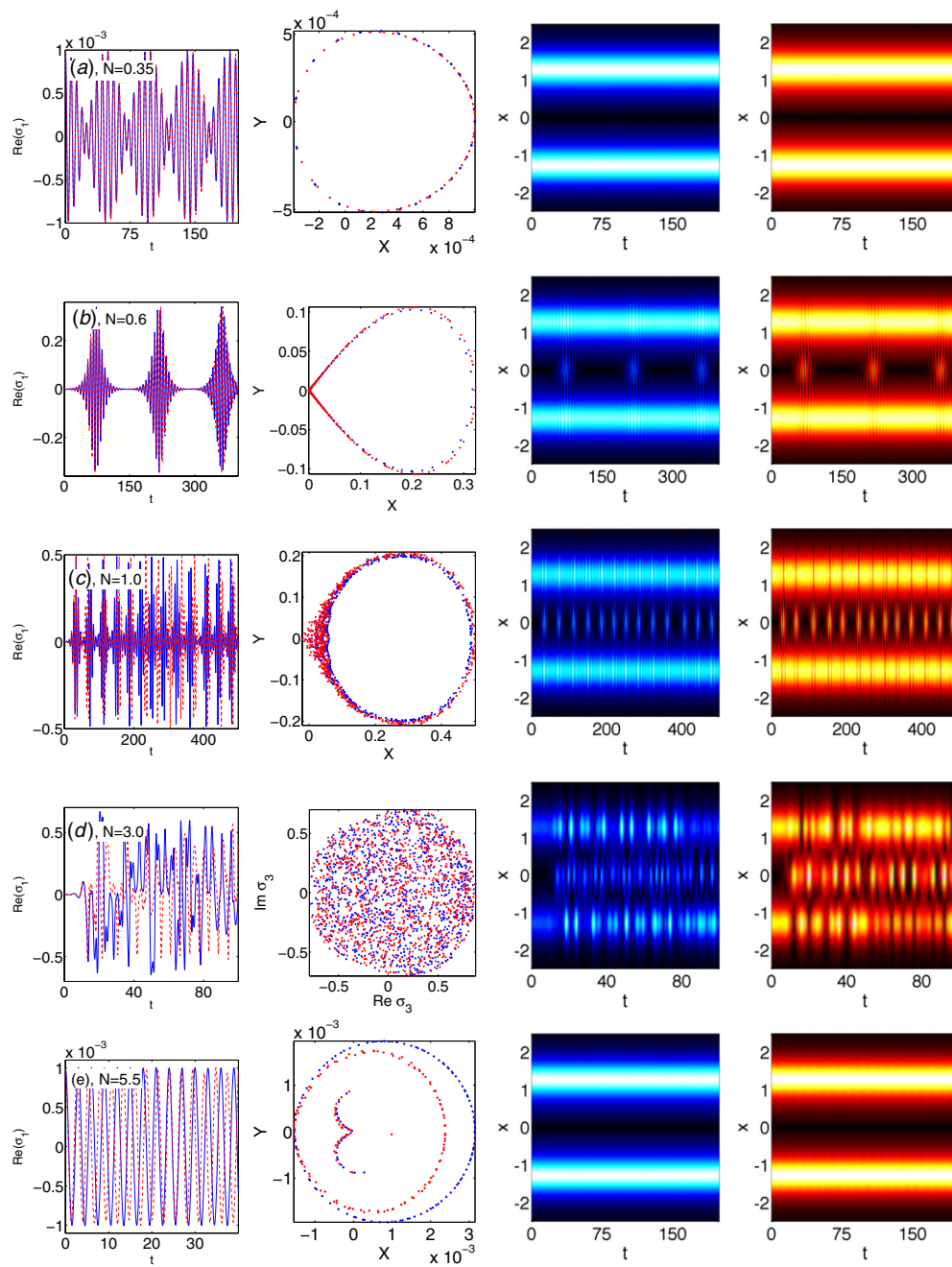


Figure 6. Simulations of ODE system (3.10) and PDE system (2.3) with initial condition of the form (3.1). The rows (a)–(e) correspond to the values of N indicated on figure 5. Column 1: $\Re\sigma_1(t)$. Column 2: Poincaré section at $\psi_1 = 0$ (except row 4, see text) with ODE solutions in blue and PDE in red. Column 3: $|u(t)|$ reconstructed from ansatz (3.8) (brighter = higher intensity). Column 4: $|u(t)|$ for computed solution of (2.3).

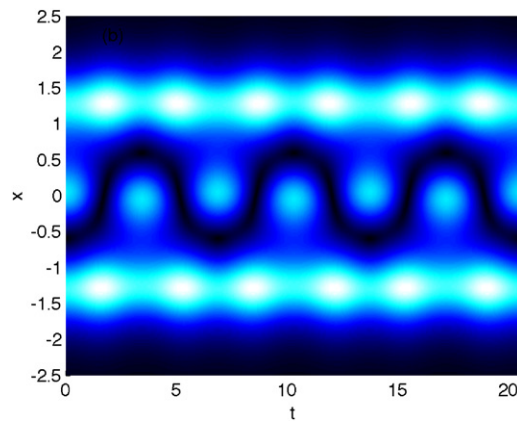


Figure 7. The field $|u_{\text{recon}}(x)|$, reconstructed from a periodic solution to (3.10) with $N = 2 > N_{\text{KC}}$.

around the center line, and a bright spot grows and decays periodically in the center well, a bright spot that is absent in the antisymmetric defect mode. A future study will look specifically at the shadowing of this ODE solution by a time-dependent solution to the NLS/GP equation (1.1).

As the system reaches the second HH bifurcation at $N \approx 4.71$ where the trivial solution regains stability, the periodic orbit does not disappear, nor does the chaotic motion shown in row (d) of figure 6. Instead, a small region around the origin appears at this amplitude, on which the solution is regular (quasiperiodic and confined to topological ellipses), and this region grows as N is further increased. This is confirmed by numerical simulation. Johansson finds similar Hamiltonian chaos when the parameters in his NLS trimer are in the unstable domain, as well as KAM-like islands [11].

6. Discussion and conclusions

While many papers, discussed in the introduction, have examined the HH bifurcation and the onset of oscillatory instabilities in nonlinear wave equations, this is the first we know of to analyze the nonlinear dynamics that arise. A pair of homoclinic orbits are found in the averaged equations, which act as skeletons for weakly chaotic dynamics. At stronger nonlinearities, chaotic orbits seem to fill the entire phase space. New families of relative periodic solutions are found in the finite dimensional model, showing a time-dependent symmetry breaking.

While the analysis presented is formal, the pieces are in place to make rigorous the conclusions, as discussed at the end of section 3.1. Kirr *et al* [4] and Marzuola and Weinstein [6] first derive finite-dimensional model equations and then prove their validity over long times. Pelinovsky and Phan [7], in contrast, derive the model equations using normal forms, which essentially combines the two steps. This normal form does not, however, exploit the Hamiltonian structure of NLS/GP. Bambusi, in a series of papers, has applied the Hamiltonian methodology of Birkhoff and Gustavson normal forms directly to NLS/GP and other wave equations, for example [29–31], proving the accuracy of these normal forms over much longer (exponential) time scales than the other methods are capable of. This work involves systems possessing only a discrete spectrum (due to trapping potentials or finite spatial domains), so that the quadratic part of the Hamiltonian can be written as an infinite series over coefficients of the eigenfunctions, and the argument of section 3.3 can be generalized straightforwardly.

These assumptions on the spectrum are also necessary for the applicability of the normal forms over such long time scales. In [32], Bambusi and Cuccagna apply the method to a Klein–Gordon equation in three spatial dimensions with a potential that vanishes at infinity, and so generalize the Birkhoff normal form to systems with a continuous spectrum. This result applies only for solutions with very small initial data, where the effect of the nonlinearity is not strong enough for the bifurcations and strongly nonlinear dynamics that we have discussed. Nonetheless, this is a promising approach for future research.

In the finite dimensional system of approximate equations near a symmetry-breaking bifurcation, derived in [4, 6], it takes one line of algebra to show the existence of the two new asymmetric solutions that are born when the bifurcation occurs. In system (3.4), the analysis is not so simple, and the new solution arising from the bifurcation appears, in its simplest form, as the equilibrium (4.8) of Hamiltonian system (3.19) that corresponds to a periodic orbit of system with Hamiltonian (3.6). Proving the existence of this periodic orbit is a straightforward application of a paper from the late 1980s by Chow and Kim [33] and will constitute the first step of a planned program to put the results of the present paper on a more rigorous footing. Beyond that, almost nothing has been proven about the semisimple indefinite HH bifurcation. One might hope to reproduce some of the many results proven for the generic case, but because the semisimple case has higher codimension, the analysis should be harder.

In numerical simulations of this system, we observe Hamiltonian chaotic motion, the underlying dynamics of which, given by system (3.6) are essentially two degree-of-freedom. Motion of such a system occurs on level sets of the Hamiltonian H which are three-dimensional manifolds in the four-dimensional phase space. Invariant tori in this system are two-dimensional subsets of these manifolds. The KAM theorem (or something very similar, see [23]) implies that most of these tori persist when $0 < (\mathcal{N} - \mathcal{N}_{\text{KC}}) \ll 1$. A two-dimensional torus separates the three-dimensional manifold, so that trajectories cannot cross from one side of the torus to the other. This implies that solutions starting near the odd-symmetric relative equilibria must remain near that point. If the linear system (2.1) is assumed to support a fourth eigenmode, with similar assumptions on the spacing of the eigenvalues, then in this weakly unstable regime, with six-dimensional phase space, solutions no longer need stay close to the equilibrium, a process known as Arnol'd diffusion [37]. Further studies are planned to investigate this possibility.

We have assumed throughout this paper that the potential $V(x)$ enjoys even spatial symmetry. The HH bifurcation we discussed depends only on assumptions (S1)–(S4) and not on this symmetry. Lacking such a symmetry, the finite-dimensional model (3.6) and its relative equilibria given in section 4.1 would be significantly more complicated, and the normal form for the HH bifurcation might no longer be semisimple. An interesting question would be to see how the dynamics change in the face of such asymmetry.

Finally, when considered as a model for an optical waveguide, the system studied here should be straightforward to implement in a laboratory setting. Discussions are underway to make this happen and will form the basis of an experimental line of research.

Acknowledgments

Thanks to Denis Blackmore, Eduard Kirr, Elie Shlizerman, David Trubatch and Michael Weinstein for useful discussions, Richard Kollar and Arnd Scheel for useful comments in response to a presentation, and Jeremy Marzuola for a careful reading of the manuscript. Thanks to the referees for their many suggestions, which have significantly improved this

paper. The code used to simulate PDE solutions is by Tomáš Dohnal. RHG was supported by NSF-DMS-0807284. This work was completed while the author was on sabbatical at Technion, the Israel Institute of Technology. He thanks them for their hospitality.

Appendix. Construction of the linear potential $V(x)$

Most other studies about the dynamics and stability of nonlinear PDEs with multi-well potentials have constructed the potential as the sum of several simpler potentials as in equations (1.3) and (1.4) [4, 6, 7, 5, 8]. This construction provides, very simply, families of potentials with nearly-multiple eigenvalues, but does not allow the control needed to construct potentials satisfying the assumptions (S1)–(V3).

Another way to proceed is to use inverse scattering methods to construct a reflectionless potential with prescribed eigenvalues $\Omega_j = -\kappa_j^2$, $j = 1 \dots n$. This process yields a potential that is unique except for n integrating factors ξ_j , which can be chosen uniquely to make $V(x)$ satisfy assumption (V3). The solution is a two-soliton solution of the Korteweg–de Vries equation [42]. This solution is most easily constructed using the Darboux transformation, which is very similar to the Bäcklund transformation, except that it yields not only the potential, but also its eigenvectors, which is useful in what follows [43, 44]. When $n = 2$, the general formula for this two-soliton is

$$V(x) = \frac{4(\kappa_2^2 - \kappa_1^2)(\kappa_2^2 \cosh 2\kappa_1 x + \kappa_1^2 \cosh 2\kappa_2 x)}{((\kappa_1 - \kappa_2) \cosh(\kappa_2 + \kappa_1)x + (\kappa_1 + \kappa_2) \cosh(\kappa_1 - \kappa_2)x)^2} \quad (\text{A.1})$$

with $\kappa_1 > \kappa_2 > 0$. This has (un-normalized) ground state and excited states

$$U_1 = \frac{\cosh \kappa_2 x}{(\kappa_1 - \kappa_2) \cosh(\kappa_1 + \kappa_2)x + (\kappa_1 + \kappa_2) \cosh(\kappa_1 - \kappa_2)x}$$

and

$$U_2 = \frac{\sinh \kappa_1 x}{(\kappa_1 - \kappa_2) \cosh(\kappa_2 + \kappa_1)x + (\kappa_1 + \kappa_2) \cosh(\kappa_1 - \kappa_2)x}$$

and frequencies $\Omega_j = -\kappa_j^2$. When $\kappa_1 = 2$ and $\kappa_2 = 1$, this potential reduces to the familiar initial condition for the KdV two-soliton $V(x) = -6\text{sech}^2 x$ with frequencies $\Omega_1 = -4$ and $\Omega_2 = -1$. Choosing $\kappa_1 = \sqrt{1 + \epsilon}$ and $\kappa_2 = \sqrt{1 - \epsilon}$, with $0 < \epsilon \ll 1$, the potential (A.1) takes the form of dual-well potential, very similar to that studied by Kirr *et al*, but with closed-form eigenvalues and eigenfunctions.

The potential $V(x)$ constructed as above with three frequencies and satisfying assumption (V3) is similar in form to that in (A.1), but with ten terms in the numerator and four in the denominator. This solution is given in the supplementary materials (available at stacks.iop.org/JPA/44/425101/mmedia), as well as a Mathematica notebook of its derivation. As the spacings between the frequencies are chosen to approach zero, the potential $V(x)$ asymptotically approaches the superposition of three identical potentials with large spacing, as studied by Kapitula *et al* [8].

References

- [1] Boyd R W 2008 *Nonlinear Optics* 3rd edn (New York: Academic)
- [2] Newell A C and Moloney J V 2003 *Nonlinear Optics (Advanced Book Program)* (Boulder, CO: Westview Press)
- [3] Pitaevskii L and Stringari S 2003 *Bose–Einstein Condensation* (Oxford: Oxford University Press)
- [4] Kirr E W, Kevrekidis P G, Shlizerman E and Weinstein M I 2008 *SIAM J. Math. Anal.* **40** 566–604
- [5] Sacchetti A 2009 *Phys. Rev. Lett.* **103** 194101
- [6] Marzuola J L and Weinstein M I 2010 *DCDS-A* **28** 1505–54
- [7] Pelinovsky D and Phan T 2011 arXiv:1101.5402v1

- [8] Kapitula T, Kevrekidis P G and Chen Z 2006 *SIAM J. Appl. Dyn. Syst.* **5** 598–633
- [9] Mayteevarunyoo T, Malomed B A and Dong G 2008 *Phys. Rev. A* **78** 53601
- [10] Kapitula T and Kevrekidis P G 2005 *Chaos* **15** 037114
- [11] Johansson M 2004 *J. Phys. A: Math. Gen.* **37** 2201
- [12] Kapitula T, Kevrekidis P G and Malomed B A 2001 *Phys. Rev. E* **63** 036604
- [13] Morgante A M, Johansson M, Kopidakis G and Aubry S 2000 *Phys. Rev. Lett.* **85** 550–3
- [14] Panda S, Lahiri A, Roy T K and Lahiri A 2005 *Physica D* **210** 262–83
- [15] Kevrekidis P G, Frantzeskakis D J, Malomed B A, Bishop A and Kevrekidis I 2003 *New J. Phys.* **5** 64
- [16] Kevrekidis P G, Malomed B A, Frantzeskakis D J, Bishop A R, Nistazakis H E and Carretero-González R 2005 *Math. Comput. Simulat.* **69** 334–45
- [17] Li L, Li Z, Malomed B A and Mihalache D 2005 *Phys. Rev. A* **72** 033611
- [18] Nistazakis H, Frantzeskakis D J and Kevrekidis P G 2007 *Phys. Rev. A* **76** 063603
- [19] Theocharis G, Weller A, Ronzheimer J P, Gross C, Oberthaler M K, Kevrekidis P G and Frantzeskakis D J 2010 *Phys. Rev. A* **81** 063604
- [20] van der Meer J-C 1985 *The Hamiltonian Hopf Bifurcation (Lecture Notes in Mathematics vol 1160)* (Berlin: Springer)
- [21] Cushman R and Rod D L 1982 *Physica D* **6** 105–12
- [22] Gaivão J P and Gelfreich V 2011 *Nonlinearity* **24** 677
- [23] Dullin H R and Ivanov A V 2005 *Phys. D* **201** 27–44
- [24] Kapitula T, Kevrekidis P G and Sandstede B 2004 *Phys. D* **195** 263–82
- [25] Kapitula T, Kevrekidis P G and Sandstede B 2005 *Phys. D* **201** 199–201
- [26] Kapitula T, Kevrekidis P G and Carretero-González R 2007 *Phys. D* **233** 112–37
- [27] Hislop P D and Sigal I M 1996 *Introduction to Spectral Theory: With Applications to Schrödinger Operators (Applied Mathematical Sciences)* (Berlin: Springer)
- [28] Wiggins S 2003 *Introduction to Applied Nonlinear Dynamical Systems and Chaos* 2nd edn (Berlin: Springer)
- [29] Bambusi D 2008 *Hamiltonian Dynamical Systems and Applications (NATO Science for Peace and Security Series B: Physics and Biophysics)* (Dordrecht: Springer) pp 213–47
- [30] Bambusi D 1999 *Math. Z.* **230** 345–87
- [31] Bambusi D and Sacchetti A 2007 *Commun. Math. Phys.* **275** 1–36
- [32] Bambusi D and Cuccagna S 2009 arXiv:0908.4548
- [33] Chow S-N and Kim Y-I 1988 *Applicable Anal.* **31** 163–99
- [34] Lahiri A and Roy M S 2001 *Int. J. Nonlinear Mech.* **36** 787–802
- [35] MacKay R 1987 *Hamiltonian Dynamical Systems* ed J M R MacKay (Bristol: Hilger) pp 137–53 (available at <http://books.google.com/books?id=a1ToPs9iZIEC>)
- [36] Luzzatto-Fegiz P and Williamson C H K 2011 *Proc. R. Soc. A* **467** 1164–85
- [37] Arnol'd V I, Kozlov V V and Neishtadt A I 1997 *Mathematical Aspects of Classical and Celestial Mechanics* 2nd edn (Berlin: Springer)
- [38] Guckenheimer J and Holmes P 1983 *Nonlinear Oscillations, Dynamical Systems, and Bifurcations of Vector Fields* (New York: Springer)
- [39] Brugnano L, Iavernaro F and Trigiante D 2009 *AIP Conf. Proc.* **1168** 715–8
- [40] Kennedy C A and Carpenter M H 2003 *Appl. Numer. Math.* **44** 139–81
- [41] Dohnal T and Hagstrom T 2007 *J. Comput. Phys.* **223** 690–710
- [42] Drazin P G and Johnson R S 1993 *Solitons: An Introduction* (Cambridge: Cambridge University Press)
- [43] Ablowitz M J, Prinari B and Trubatch A D 2004 *Discrete and Continuous Nonlinear Schrödinger Systems* (Cambridge: Cambridge University Press)
- [44] Matveev V B and Salle M A 1991 *Darboux Transformations and Solitons* (Berlin: Springer)